OREGON GEOLOGY

published by the
Oregon Department of Geology and Mineral Industries

VOLUME 59, NUMBER 3 MAY/JUNE 1997

IN THIS ISSUE:

OREGON GEOLOGY

(ISSN 0164-3304)

VOLUME 59, NUMBER 3 MAY/JUNE 1997

Published bimonthly in January, March, May, July, September, and November by the Oregon Department of Geology and Mineral Industries. (Volumes 1 through 40 were entitled *The Ore Bin*.)

Main Office: Suite 965, 800 NE Oregon Street # 28, Portland 97232, phone (503) 731-4100, FAX (503) 731-4066.
Baker City Field Office: 1831 First Street, Baker City 97814, phone (541) 523-3133, FAX (541) 523-5992.
Mark L. Ferns, Regional Geologist.
Grants Pass Field Office: 5375 Monument Drive, Grants Pass 97526, phone (541) 476-2496, FAX (541) 474-3158.
Thomas J. Wiley, Regional Geologist.
Mined Land Reclamation Program: 1536 Queen Ave. SE, Albany 97321, phone (541) 967-2039, FAX (541) 967-2075.
Gary W. Lynch, Supervisor.
The Nature of the Northwest Information Center: Suite 177, 800 NE Oregon Street # 5, Portland, OR 97232-2162, phone (503) 872-2750, FAX (503) 731-4066, Donald J. Haines, Manager.

Periodicals postage paid at Portland, Oregon. Subscription rates: 1 year, $10; 3 years, $22. Single issues, $3. Address subscription orders, renewals, and changes of address to *Oregon Geology*, Suite 965, 800 NE Oregon Street # 28, Portland 97232. **POSTMASTER: Send address changes to *Oregon Geology*, Suite 965, 800 NE Oregon Street # 28, Portland 97232-2162.**

Oregon Geology is designed to reach a wide spectrum of readers interested in the geology and mineral industry of Oregon. Manuscript contributions are invited on both technical and general-interest subjects relating to Oregon geology. Two copies of the manuscript should be submitted. If manuscript was prepared on common word-processing equipment, a file copy on diskette should be submitted in place of one paper copy (from Macintosh systems, high-density diskette only). Graphics should be camera ready; photographs should be black-and-white glossies. All figures should be clearly marked; figure captions should be together at the end of the text.

Style is generally that of U.S. Geological Survey publications. (See USGS *Suggestions to Authors*, 7th ed., 1991, or recent issues of *Oregon Geology*.) Bibliography should be limited to references cited. Authors are responsible for the accuracy of the bibliographic references. Include names of reviewers in the acknowledgments.

Authors will receive 20 complimentary copies of the issue containing their contribution. Manuscripts, letters, notices, and meeting announcements should be sent to Beverly F. Vogt, Publications Manager, at the Portland office (address above).

Cover photo

Oregon coast south of Coquille Point and the city of Bandon in Coos County. This Oregon Department of Transportation photo from about 1970 shows one example of some 25 mi of marine terrace exposures that were examined for evidence of liquefaction related to earthquakes in the past. Some sites mentioned in the article beginning on the next page are located north and south of this particular terrace.

Oregon tsunami hazard signs officially adopted by California, Washington, Alaska, and Hawaii

Undersea earthquakes can cause tsunamis. These seismic sea waves have hit the coast of the Pacific Northwest in the past and will again in the future. Coastal residents and visitors have to be alerted to the hazard so they know what to do to protect themselves.

In 1994, representatives from the Oregon Department of Geology and Mineral Industries, Department of Transportation, Land Conservation and Development, Parks and Recreation, and Oregon State University Extension Sea Grant searched for an international warning symbol for tsunamis and could not find one.

So they asked Oregon State University Extension and Experiment Station Communications artist Tom Weeks to make one, and he created the bright blue tsunami hazard zone and tsunami evacuation route signs that are now showing up all along the Oregon coast.

At its March 4, 1997, meeting in Seattle, the Tsunami Hazard Mitigation Federal/State Steering Group voted unanimously to adopt the Oregon signs as official tsunami hazard zone and evacuation route signs for California, Washington, Alaska, and Hawaii. This means that anyone visiting the beaches in any of those states will see the same signs warning them of this hazard.

The blue-and-white reflective signs are manufactured by the Oregon Department of Transportation and come in several sizes. The round evacuation route sign features a tsunami wave and is available in 12-, 18-, and 24-inch diameter sizes. A second sign with a white arrow on a blue background is placed below the evacuation route sign to show which way to go to safely escape a tsunami.

The rectangular tsunami hazard zone sign shows a person running up a hill to escape the tsunami wave and says, "In case of earthquake, go to high ground or inland." The hazard zone sign, which is to be placed in low-lying areas that are vulnerable to tsunamis, also comes in three sizes: 15×12, 22½×18, and 30×24 inches. Signs may be placed only in locations agreed upon by local and/or state governmental authorities and may be purchased by calling Orville Gaylor, Oregon Department of Transportation, 503-986-3603. □

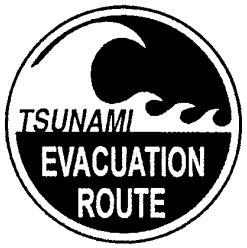

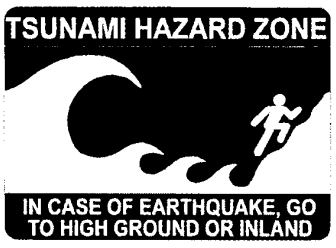

Coseismic paleoliquefaction evidence in the central Cascadia margin, USA

by Curt D. Peterson, Portland State University, Portland, Oregon 97207-0751; and Ian P. Madin, Oregon Department of Geology and Mineral Industries

ABSTRACT

Approximately 40 km of late Pleistocene marine terrace exposures on the coasts of Oregon and Washington were surveyed for evidence of coseismic paleoliquefaction. Clastic dikes and sills and other fluidization features are reported from 25 localities that are screened for likely seismic origins of fluidization. At least 11 of the localities demonstrate erosional truncation and burial of the fluidization features, implying that corresponding paleoliquefaction was syndepositional with the marine highstands. Features interpreted to reflect strong shaking include cobble plumes (2 sites), lateral spreads (2 sites), and large clastic dikes at least 20 cm wide (10 sites).

Inland from the coast, late Holocene deposits of the upper Columbia River valley (Portland to Bonneville) were surveyed for paleoliquefaction evidence that might correspond to the proposed A.D. 1700 Cascadia earthquake records reported for the lower Columbia River valley. About 1 km of cutbank exposures from eight islands was examined for evidence of late prehistoric and/or historic liquefaction in the upper Columbia River valley. All but one island locality showed evidence of small clastic dikes (generally 3–6 cm maximum width) in late prehistoric deposits but no apparent fluidization in surficial "historic" deposits.

The age of the fluidization event(s) in the upper river valley is bounded by upper radiocarbon dates from two islands (250±70 and 260±50 RCYBP [radiocarbon years before present]) and by lower, dike-intruded "tephra" layers (410±70 RCYBP). These fluidization features are tentatively correlated to paleoliquefaction in the lower Columbia River that has been attributed to the last Cascadia earthquake, circa A.D. 1700. If verified, these correlations would extend the known liquefaction from a Cascadia subduction-zone earthquake to a distance of at least 150 km due east from the coast, along the Columbia River.

INTRODUCTION

The potential for strong ground motion associated with interplate earthquakes in the Cascadia margin (Figure 1) has been widely debated. A lack of consensus on this issue has led planners to rely on probabilistic models based on a range of earthquake scenarios (Geomatrix Consultants, Inc., 1995). Another approach to estimating the potential strength of shaking is provided by the geologic record of paleoliquefaction. Local ground accelerations and duration of sufficient magnitude to damage unreinforced structures should also produce clastic dikes and other similar features

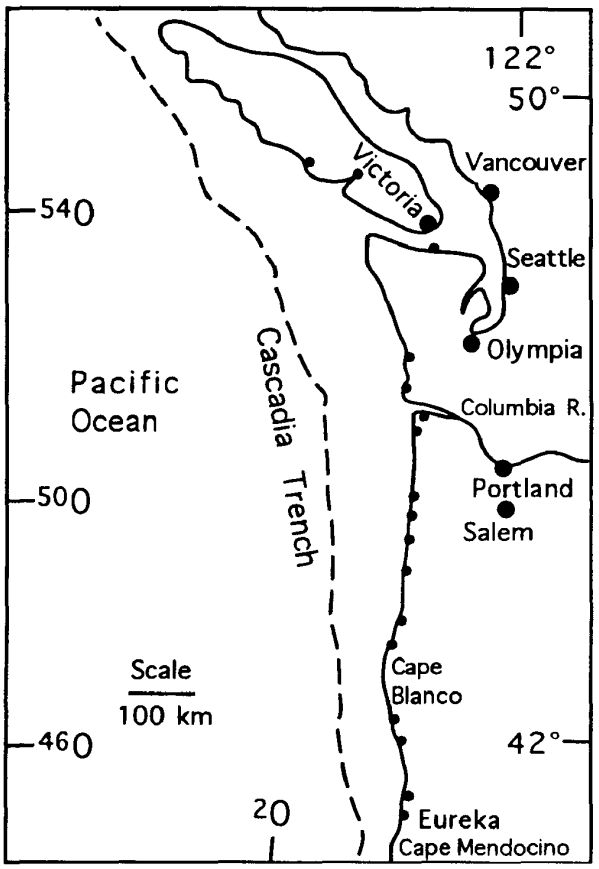

Figure 1. Map showing the Cascadia margin from Vancouver Island to Cape Mendocino, including the trench (dashed line), shoreline (solid line), Columbia River (solid line), major cities (large solid circles), and smaller coastal cities (small solid circles).

in susceptible deposits (Youd, 1991). A lack of such features would argue against, but not rule out, strong shaking during the period of record. In this regard, paleoliquefaction evidence serves as an indicator of the strength of prehistoric ground motion.

It is possible, but more difficult, to use paleoliquefaction evidence to confirm the magnitude of earthquakes in early historic time (Saucier, 1989; Tuttle and Seeber, 1991; Obermeier, 1996). This requires discrimination between fluidization from coseismic and aseismic mechanisms. This is aided by (1) ruling out depositional environments that foster rapid autocompaction or hydraulic pumping, and (2) establishing spatial trends in the distribution of fluidization

features that correspond to historic seismic sources (Obermeier, 1996). Peak ground accelerations and corresponding soil liquefaction should diminish with increasing distance from the earthquake epicenter. Site-specific conditions of ground motion amplification and deposit susceptibility to fluidization can strongly influence the local development of coseismic liquefaction (National Research Council, 1985). Therefore, ground motion attenuation must be established over large distances to rule out local effects from wave focusing and site amplification.

Paleoliquefaction analysis of prehistoric earthquakes can be a difficult undertaking in settings that contain multiple earthquake sources. For example, subduction zones, such as the Cascadia subduction zone (CSZ) can include interplate (megathrust) sources, deep intraplate (Benioff-Wadati zone) sources, and shallow upper plate (crustal) sources (Geomatrix Consultants, Inc., 1995). These factors limit the use of paleoliquefaction evidence to independently establish the magnitude of prehistoric earthquakes in subduction zones. On the other hand, a lack of substantial fluidization evidence in susceptible deposits would provide a strong argument against large-magnitude earthquakes from any source within the subduction zone.

In this paper, we report on the nature, scale, and distribution of paleoliquefaction features in late Quaternary coastal and fluvial-tidal deposits of the central Cascadia margin (Figure 1). These features are observed in late Pleistocene marine terraces of the Oregon and southern Washington coasts (Peterson and Madin, 1992) and in latest Holocene deposits that are exposed in island cutbanks of the Columbia River (Obermeier and others, 1993; Atwater, 1994; Siskowic and others, 1994; Obermeier, 1995). The Pleistocene marine terraces range from 60 to 130 km in distance from the deformation front (base of the continental slope), as a function of their position on the coast. The Columbia River paleoliquefaction sites range from 30 to 150 km inland from the coast or about 150–260 km landward of the deformation front.

The fluidization features observed in the late Pleistocene coastal terraces have been analyzed for size, nature of source beds, and site-specific criteria to help discriminate between coseismic and aseismic origins. The late Holocene liquefaction sites in the Columbia River deposits have been analyzed for potential correlation to the last Cascadia dislocation event at about A.D. 1700. The results of these analyses are used to test whether strong shaking associated with large-magnitude earthquakes (M_W 8 range) can be discounted in the Cascadia subduction zone on the basis of the existing paleoliquefaction evidence.

BACKGROUND

Sediment fluidization and seismic liquefaction

Fluidization of saturated sediments occurs when unconsolidated grains in source beds are compacted into denser packing structures. The escaping pore fluid raises hydrostatic pressure, thereby locally fluidizing the unconsolidated deposits. Particle resettlement in source beds can occur from overburden pressure or strong gradients in pore pressure (aseismic liquefaction) or from cyclic shear stress through shaking (coseismic liquefaction). Sand deposits are generally more susceptible to fluidization than either gravel or cohesive mud (Seed and Idriss, 1982; Seed and others, 1985; Stokoe and others, 1988). Finally, the effects of fluidization are often most apparent directly under low-permeability capping layers (e.g., mud), where ascending pore-pressure fronts are locally enhanced (Figure 2; Fiegel and Kutter, 1994).

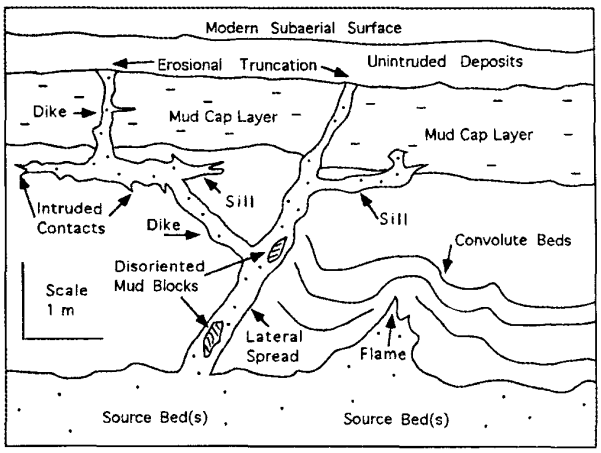

Figure 2. Drawing of subsurface fluidization features including clastic dikes and sills and flames. Internal structures include intruded contacts with host deposit and disoriented mud blocks in sandy matrix. Fluidization features such as clastic sills are often enhanced under thin capping deposits of mud overlying thick source beds of sand.

The factors that favor the development of fluidization features include (1) shallow overburden, (2) thin capping layers of impermeable deposits, and (3) thick source beds of well-sorted sand below groundwater level. On the other hand, the development of fluidization discharge features is inhibited by high lithologic pressure, containment of elevated pore pressure, and small volumes of available pore fluids. Even under "favorable" conditions the development of clastic dikes and sills can vary substantially, to the point of local absence within an outcrop. This variability in fluidization response might reflect small changes in grain packing, permeability, or bed shear strength.

As previously noted, the discrimination between coseismic and aseismic mechanisms of fluidization can be inconclusive, based on a single feature or even a single locality. For this reason, depositional environments that are associated with episodic autocompaction and/or hydraulic pumping should be ruled out for paleoseismic analysis. More specifically, aseismic fluidization can occur from rapid sedimentation rates, slope failures, artesian springs, rapid changes in groundwater saturation, and/or surf pounding, among others (Kolb, 1976; Nataraja and Gill, 1983; Holzer and Clark, 1993).

Stratigraphic evidence is very useful in constraining interpretations of the mechanisms of fluidization. Fluidization features that cut vertically through overlying strata of different depositional environments suggest coseismic origins. The strongest arguments for coseismic liquefaction come from large-scale spatial trends in the abundance and scale of fluidization features. Regional trends or continuities of paleoliquefaction sites that cross through different depositional environments imply a regional response to seismic shaking (Obermeier, 1996). In rare cases, the timing of fluidization can be tied directly to other paleoseismic indicators, such as abrupt regional subsidence, as shown later in this paper.

Post-earthquake field surveys usually rely on ground surface observations of deposits vented from sand volcanoes, i.e., sand blows and boils or sand-filled fissures, to demonstrate coseismic liquefaction. However, subsurface fluidization features are more likely to be preserved in the geologic record (Walsh and others, 1995). These features typically include clastic dikes, sills, pipes, or cones with widths of a few centimeters to several decimeters (Figure 2). The widest dikes (greater than 50 cm in width) are probably associated with lateral spreads from slope failures.

Fluidized injection features are commonly bounded by intruded (irregular) contacts with their host deposits. These contacts are sharply defined when sands are intruded into mud. The internal structures of fluidization features can include pseudo-shear bedding or laminae, grading, or particle orientation parallel to injection flow (Peterson, 1968). Inclined mud clasts or pebbles that are supported by structureless matrix are also good clues to the recognition of sediment remobilization by fluidization (Figure 2). Although not necessarily of fluidization origin, the presence of convolute beds and/or the absence of primary bedding are common indicators of potential paleoliquefaction.

A note to the reader: We use the terms "fluidization" and "liquefaction" to represent liquefaction from either aseismic or coseismic mechanisms, i.e., undifferentiated. Where abundance, regional continuity, and/or stratigraphic evidence of fluidization imply probable earthquake origins, we use the term "coseismic liquefaction."

Prehistoric liquefaction sites

An early argument against coseismic subduction in the central Cascadia subduction zone was the lack of reported fluidization features in coastal deposits. However, a preliminary search of late Pleistocene marine terraces in 1989 and 1990 showed evidence of possible coseismic fluidization in the central Cascadia margin (Peterson and others, 1991b; Peterson and Madin, 1992). Paleoliquefaction sites were found in beach, dune, and estuarine deposits from exposed sea cliffs near Gold Beach, Coos Bay, Newport, Willapa Bay, and Kalaloch (Figure 3). These paleoliquefaction sites and others in the late Pleistocene marine terraces are further described in this paper.

Evidence of fluidization in late Holocene deposits of the central Cascadia coast was first reported from the Copalis River estuary (Figure 3) (Atwater, 1992). Large-scale dikes and sills (20-cm thickness) at this site vented sand onto a paleomarsh surface, dated at 900–1,300 radiocarbon years before present (RCYBP). Unlike the bays to the south, the Copalis estuary did not experience coastal subsidence during the interval from 900 to 1,300 yr B.P., leaving some doubt as to the mechanism of fluidization at this site (Atwater, 1992). Additional late Holocene paleoliquefaction sites have been reported from the Cape Blanco area (Kelsey, and others, 1993) and the Umpqua and Siuslaw Bays of south-central Oregon (Briggs, 1994) and in small tributaries to Grays Harbor in Washington (Obermeier,

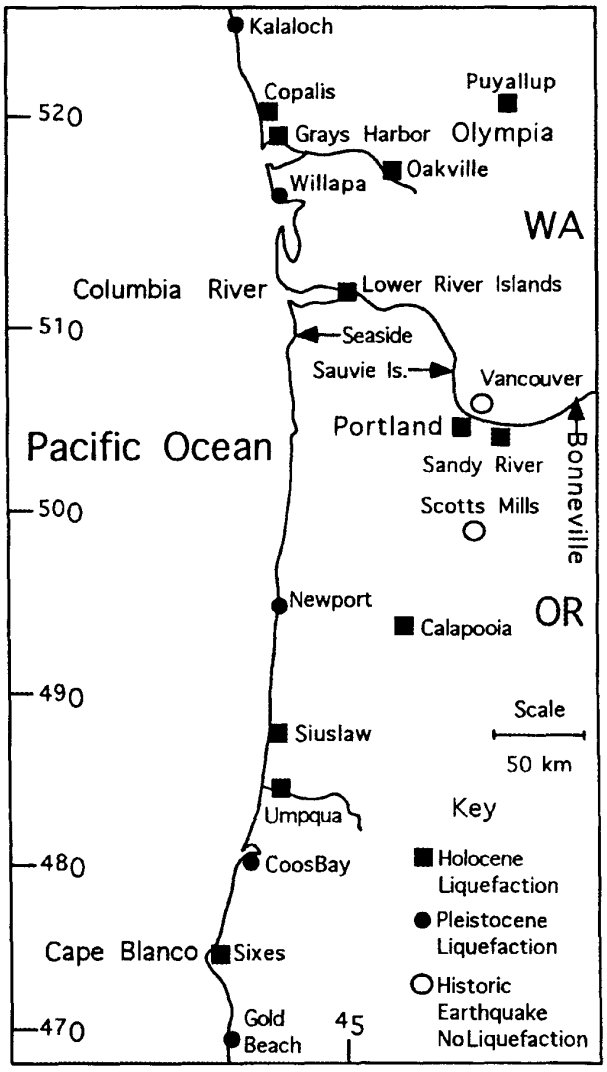

Figure 3. Map of reported liquefaction sites on the coast and at inland sites of the Cascadia margin. Solid squares represent reported Holocene coseismic-liquefaction sites. Solid circles represent reported late Pleistocene liquefaction sites. Open circles represent historic earthquakes (M_W 5) with no reported liquefaction.

1995). However, these late Holocene sites are located in small bays or creeks, and the evidence of paleoliquefaction is limited to short outcrops or subsurface cores. The potential earthquake sources responsible for these late Holocene coastal sites have yet to be rigorously established.

The most conclusive evidence of paleoliquefaction produced by a prehistoric CSZ earthquake is that observed in the lower Columbia River (Obermeier and others, 1993). Clastic dikes now exposed in river banks of small islands in the lower Columbia River estuary (Figure 3) vented sand onto wetland surfaces (Obermeier, 1995) that subsided (contemporaneously) with the last Cascadia earthquake, circa A.D. 1700 (Atwater, 1987; Darienzo, 1991). Paleoliquefaction evidence in exposed cutbanks has been traced up the Columbia River to the Sandy River delta, east of Portland (Siskowic and others, 1994; Vockler and others, 1994). Preliminary findings that tie these records of paleoliquefaction in the upper river valley to the last CSZ earthquake are discussed in this paper.

The discovery of late Holocene liquefaction sites in the upper Columbia River valley has lead to reconnaissance searches of other localities in the forearc basins for evidence of paleoliquefaction (Figure 3). Small clastic dikes have been observed in shallow late Holocene deposits exposed in river banks of the Chehalis River near Oakville, Washington, and most recently in the Calapooia River of the southern Willamette Valley, Oregon (Obermeier, 1995; Obermeier, unpublished data, 1995). By comparison, larger clastic dikes cut Missoula flood deposits (12–13 Ka) in several Portland basin localities (I.P. Madin, unpublished data, 1995). Additional work is needed to discriminate between potential local sources and regional sources of seismicity for the paleoliquefaction events recorded in forearc basin localities.

Historic liquefaction in coastal sites

Liquefaction was induced by a small (M_W 7.1) coastal earthquake that occurred in the CSZ in April 1992 at Cape Mendocino (Figure 1). Although the origin of this thrust earthquake is controversial, its focus is reported to have occurred at a depth of 10 km within the Cape Mendocino triple junction (Michael and others, 1992). Two strong aftershocks (M_W 6.6 and 6.7) occurred on separate faults about 20 km offshore. The small rupture plane (about 300 km^2) of the main shock produced local peak accelerations of at least 0.5 *g* for several seconds (Oppenheimer and others, 1993). The aftershocks produced comparable accelerations. Small sand blows from the main shock and/or aftershocks were found within a radius of about 30 km from the epicenter (Prentice and others, 1992).

Other surface expressions of the 1992 Cape Mendocino earthquake include small landslides on steep slopes and localized coastal uplift (1–1.5 m) near the epicenter (Jayko and others, 1992). With the exception of one lateral spread (0.5-m width), no extensive dike fields, fissures, or large-scale sand geysers were reported in the area. The liquefaction features observed within the epicentral region (20-km radius) of this M_W 7 subduction-zone earthquake can be generally characterized as relatively small in scale and sparse in distribution.

By comparison, an inland earthquake in the Puget Sound area of southern Washington did result in substantial liquefaction in susceptible soils, such as those in the Puyallup valley (Figure 3) (Shulene, 1990). Two earthquakes, one each in 1949 (M 7.0) and 1965 (M 6.5) originated from deep intraplate (Benioff-Wadati zone) sources. Whereas sand blows in the City of Puyallup were widely reported for the 1949 earthquake, they were less common for the 1965 event. Geotechnical site analyses (Palmer, 1990) suggest that critical accelerations of the local source beds fall between the peak ground accelerations (PGA) estimated for the 1949 event (0.17 *g*) and the 1965 event (0.11 *g*) in the Puyallup valley. The Puyallup valley is located roughly 65 km from the two different epicenters, so the unequal liquefaction response is attributed to the differences in event magnitudes (Palmer, 1990).

The Portland basin (Figure 3) has experienced several historic earthquakes in the range of M 4–5, including the largest recorded earthquake (1962) with a magnitude estimate of up to 5.5 (Bott and Wong, 1993). The 1962 earthquake produced peak ground accelerations of 0.08–0.10 *g* in downtown Portland, located about 15 km to the southwest of the proposed epicenter in Vancouver, Washington (Yelin and Patton, 1991). Sand blows were not reported for any of the historic earthquakes in the Portland area (I.G. Wong, oral communication, 1995). However, thorough searches for such features were probably not undertaken at the time of the events. Preliminary results of our ongoing searches for historic coseismic liquefaction in river cutbanks of the Portland basin are reported in this paper.

The most recent earthquake in the Portland-Willamette Valley area (Scotts Mills, M 5.6) occurred in 1993 (Figure 3). This short-duration earthquake (main shock about two seconds) was located at about 13–15 km depth (Nabelek and Xia, 1995) and probably reached peak ground accelerations of 0.11–0.12 *g* near the epicenter (Madin and others, 1993). A search of roadsides, river banks, and pond margins did not yield any surface evidence of slumps, sand blows, or fissures near the earthquake epicenter. Trenches cut into small sand bars of the Pudding River near Scotts Mills showed no evidence of liquefaction. These observations are consistent with the relatively small magnitude of this most recent event, which did cause local damage to some unreinforced structures (Black, 1996).

METHODS OF RECONNAISSANCE SURVEYS

Late Pleistocene coastal terrace outcrops

Reconnaissance surveys of paleoliquefaction evidence in late Pleistocene coastal deposits of Oregon and Washington were conducted for several weeks of each summer from 1989 to 1992. The uplifted late Pleistocene deposits are well exposed in sea cliffs, bay cliffs, and/or road cuts. In this reconnaissance survey, the youngest (lowest) locally ex-

posed terrace was generally examined for possible evidence of coseismic liquefaction. The age of the lowest terrace varies along the central Cascadia margin due to differential uplift but probably ranges between 80 and 125 Ka in age (Florer, 1972; Kennedy and others, 1982; Kelsey, 1990; McInelly and Kelsey, 1990; Muhs and others, 1990; Mulder, 1992; Ticknor, 1993; Clifton, 1994).

Three areas of the central Cascadia margin were chosen for marine terrace surveys, including (1) Kalaloch and Willapa Bay in southern Washington, (2) Netarts to Alsea Bay in central Oregon, and (3) Coos Bay to Cape Blanco in southern Oregon (sites T1–T25, Figure 4; data summary in Table 1). These areas represent different distances from the trench (Figure 1) and possibly different distances from the megathrust locked zone (Geomatrix Consultants, Inc., 1995). Multikilometer reaches within the study areas were selected for beach- and bay-cliff surveys largely on the basis of ease of accessibility. A total of about 32 km of terrace deposit exposures was examined for possible evidence of fluidization features. This total corresponds to about 10 km, 14 km, and 8 km, respectively, for the the north, central, and south study areas. The distance of road-cut exposures examined in the Coos Bay area was not logged but probably exceeds 5 km. Terrace localities with apparent clastic dikes and/or sills at least 10 cm wide were noted for subsequent examinations. No attempt was made to normalize the frequency of fluidization features by outcrop length, height, or lithology. Liquefaction localities that showed evidence of (1) landsliding, (2) loading by colluvium overburden, and/or (3) extensive groundwater leaching were abandoned. Such localities could be influenced by aseismic mechanisms of fluidization (see "Background" section above).

About two dozen coastal localities were measured and photographed for the form, size, and stratigraphic development of fluidization features. These representative localities were selected on the basis of (1) observed dikes or sills of at least 10-cm width or (2) proximity to mapped Quaternary structures (upper plate faults or folds) in the southern study area. Field logs from the localities include estimates of outcrop length, depositional environment, and the lithologies

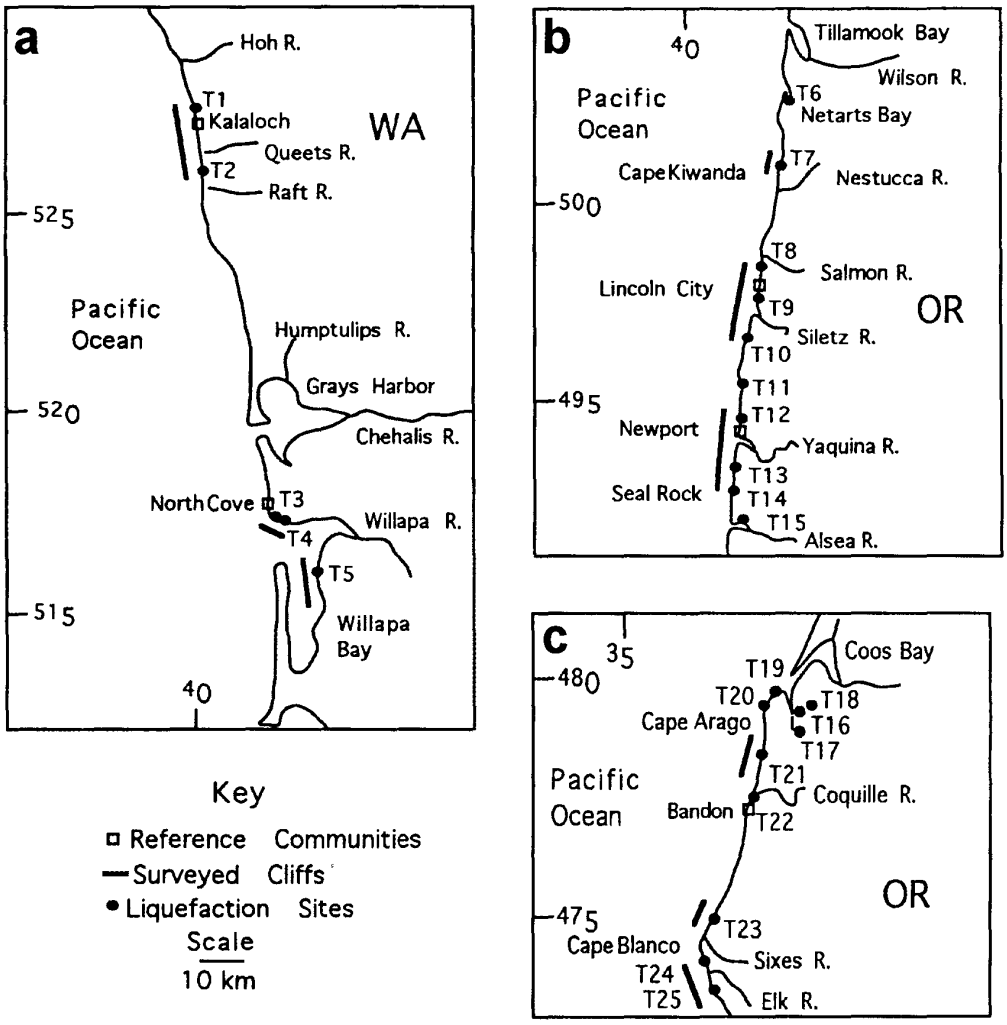

Figure 4. Maps of late Pleistocene paleoliquefaction sites (T1–T25, solid circles) in coastal marine terraces: a–north study area, b–central study area, c–south study area in the central Cascadia margin.

These areas were picked on the basis of representative distances from the trench. Specific beach-cliff traverses within the study areas were picked on the basis of known exposure of marine terrace deposits and ease of accessibility.

of the source beds, host deposits, and capping deposits. Particular attention was paid to localities that showed erosional truncation and subsequent burial of clastic dikes and sills or convolute beds. The burial of these truncated features constrains the timing of fluidization to the general period of deposition during the corresponding marine highstand (see "Discussion" section below).

For the purposes of this study only the largest fluidization features, i.e., plumes, lateral spreads, dikes, and sills, were measured at each locality. Clastic dikes were defined here as injection-conduit features, i.e., tabular bodies of sandy material, with apparent dips of at least 45° from horizontal in the plane of the outcrop. Some dikes were observed to widen at their base, so maximum dike width was taken from about the middle of the largest dike observed in the outcrop. Maximum sill width was taken from the largest sill that was not associated with a sill-dike juncture in the plane of the outcrop. Measurements of the widths of the largest features, i.e., cobble plumes and lateral spreads, were arbitrarily limited to 100 cm. Some of the largest features, those wider than 1 m, appear to contain multiple shear boundaries, which made it difficult to establish the width of a single feature or event. Due to the limited vertical exposures of most outcrops, typically less than 5 m in sea cliffs and less than 3 m in road cuts, the maximum lengths of clastic dikes are rarely exposed. Therefore the measurements of dike lengths reported here are minimum lengths, as exposed in the outcrop.

Late Holocene cutbanks of Columbia River islands

In 1991, initial observations of possible paleoliquefaction features were made in late Holocene deposits of the lower Columbia River area. Convolute bedding was found in cutbanks of a drainage ditch in Sauvie Island, near Portland, and fluidized sands were found beneath the youngest buried marsh deposit exposed in cutbanks of Neawanna River, north of the S Avenue bridge in Seaside, Oregon (Figure 3). A regional survey of the lower Columbia River islands in 1992 resulted in the discovery of widespread paleoliquefaction features (Obermeier and others, 1993). It was followed up in 1993 with a more thorough search for fluidization features and some subsurface geotechnical testing (Atwater, 1994; Obermeier, 1995).

Exposed cutbanks of these islands in the lower Columbia River valley were surveyed at low tides for evidence of vertical dikes cutting through capping layers of mud. In the westernmost islands, some dikes vented sand onto a paleowetland surface (peaty mud) that had abruptly subsided and had been buried by lower intertidal muds. Several of the island sites also show dikes cutting a thin tephra layer, located about half a meter below the paleosurfaces of sand venting. Samples for radiocarbon dating and tephrachronology were collected from these outcrops to establish the relative ages of the fluidization associated with the wetland subsidence. Subsurface deposits from islands in the lower reaches of the Columbia River have been examined for paleoliquefaction evidence by vibracoring (Craig and others, 1993; Peterson and others, 1994).

Cutbanks in islands and floodplains of the Columbia River east of Portland were surveyed for liquefaction evidence during the summers of 1993–1995. Upriver from Portland, the cutbanks were selected on the basis of active channel erosion into deposits that are rooted by old cottonwood trees with trunk diameters greater than 1 m. Tree-ring counts on sawn stumps indicate that these old trees are approximately 50–100 yr in age. Thus, the underlying deposit surfaces should predate most dredge-and-fill operations on the river.

Convolute bedding and small dikes and sills were traced upriver along cutbanks from Government Island, just east of Portland, to Pierce Island, just downstream from the Bonneville Dam (Figure 3). Wood fragments from horizons immediately above intruded dikes or sills were collected from the Sandy River delta and Pierce Island for radiocarbon dating. Apparent "tephra" horizons cut by the fluidization features were collected at the Sandy River delta and at Reed Island for petrographic and geochemical analysis. A preliminary report on liquefaction susceptibility in the Sandy River delta has been presented by Anderson and others (1994).

RESULTS

Late Pleistocene paleoliquefaction

Kalaloch to Willapa Bay (Figure 4a)

Sea cliffs north and south of Kalaloch, Washington, contain multiple liquefaction sites in a low marine terrace. This terrace is thought to be correlative with the 80-Ka marine highstand (Florer, 1972). This part of the coast is deformed by faults and folds (Rau, 1973), apparently representing an onshore expression of the accretionary wedge. Just north of Point Brown (site T1), beach cobble imbrication demonstrates multiple convection plumes (Figure 5a). Convection structures are known from cyclic stress loading of dry granular materials (Jaeger and others, 1996) but have not been reported previously for coseisimic disturbance sites. Small clastic sand dikes and sills are intruded into lagoonal muds that are located stratigraphically above the disturbed beach cobble deposits at this site. The presence of the small clastic dikes (5 cm wide) in lagoonal mud layers above the cobble plumes at site T1 argues against fluidization from surf pounding. However, additional work to test the interpreted coseismic origin of the imbricate cobble convection structures is warranted.

Larger dikes (20 cm wide) occur near Whale Creek (site T2). They are erosionally truncated, indicating that paleoliquefaction events at these sites were syndepositional with the period of marine highstand deposition. Relatively minor liquefaction features, e.g., small sand dikes and sills, were found in coarse-grained glacial outwash deposits between Whale Creek and the Queets River.

The accretionary wedge is assumed to be well offshore off Willapa Bay in southernmost Washington. Lateral

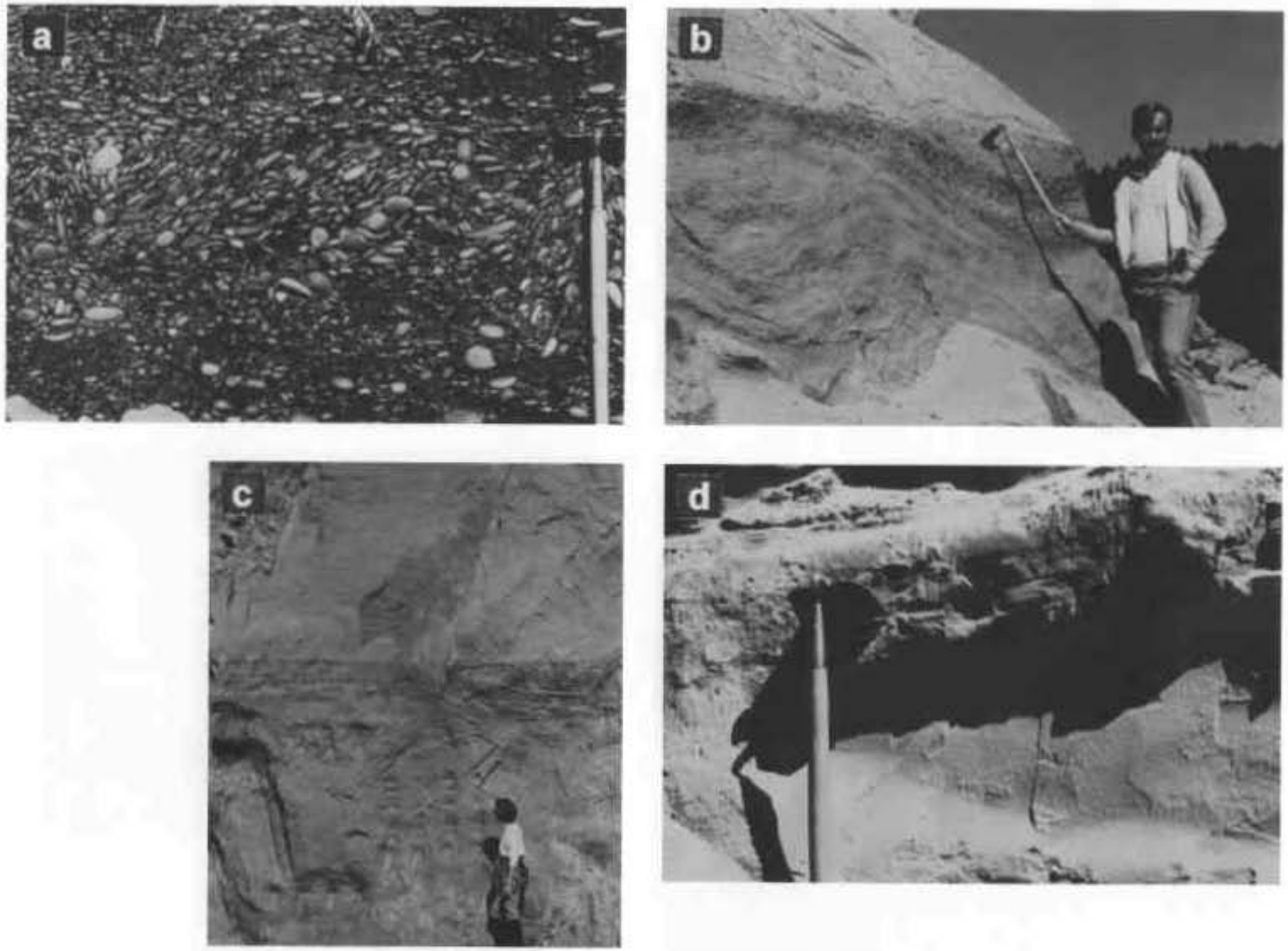

Figure 5. Photographs of (a) cobble plumes at Point Brown, Wash. (site T1) (hoe handle is 40 cm long); (b) 10-m vertical section of tidal inlet deposits dismembered by lateral spreads, sills, dikes, and convolute bedding at the North Cove quarry (site T3); (c) 40-cm-wide dike feeding a flame structure intruded into overlying host deposits (also site T3); note that two episodes of syndepositional paleoliquefaction are separated by the erosional truncation of fluidization features in the underlying source beds); (d) a clastic sill (0.5 m wide) intruded into estuarine mud deposits in a young (80 Ka) terrace inset in Willapa Bay (site T5).

spreads and large dikes (40 cm wide) occur at the North Cove quarry (site T3) in late Pleistocene terrace deposits (at least 125 Ka) at the north end of Willapa Bay (Figure 5b). These deposits of tidal-inlet sand (10–20 m thick) over gravel (10 m thick) show multiple episodes of liquefaction. At least two liquefaction events are separated by erosional truncation of fluidization features and subsequent flame injection through the erosional contact (Figure 5c). The flame is intruded into overlying beds that are undisturbed, which implies that the paleoliquefaction did not arise from channel-bank slumping. This paleoliquefaction locality appears to extend at least 0.5–1 km southwest to site T4, where rare clastic dikes (up to 20 cm wide) in tidal-flat facies are fed by convolute source beds of sand at several meters depth below the rare dikes (Table 1). Sills are more abundant than dikes (ratio greater than 10:1) in these layered tidal-flat deposits.

Clastic sills and rare dikes are found in the lower (80–120 Ka) terraces surrounding Willapa Bay, such as at site T5 (Figure 5d). The scale and abundance of paleoliquefaction features in the Willapa Bay terraces diminish to the south, where the late Pleistocene deposits are dominated by mud or muddy sand facies (Clifton, 1994). Muddy flowage structures (as described below for Netarts Bay) were observed in about a dozen sites in a 5-km traverse of bay terraces along the eastern shore of Willapa Bay.

Netarts to Alsea Bay (Figure 4b)

Late Pleistocene marine terraces along the eastern shore of Netarts Bay are dominated by thin-bedded mud and buried peats (Mulder, 1992). Thin layers of channel sand feed clastic dikes (up to 20 cm thick) that cut through capping layers of mud and peat. However, the dominant forms of liquefaction at the Netarts locality (site T6) are muddy flowage structures. The fluidization of these viscous mud deposits is demonstrated by flow banding (shear orientation) of organic fragments in the convolute mud layers. The injected mud is sometimes confined between deformed, but intact, peaty layers.

Eight paleoliquefaction sites exposed in sea cliffs were

Table 1. Paleoliquefaction localities in late Pleistocene marine terraces. For locations, see Figure 4

Site name (number T-)	UTM coordinates	Exposure length (m)	Depositional setting	Maximum fluidization	Feature width (cm)	Feature length (m)	Source bed lithology	Host deposit lithology	Capping bed lithology	Accessory features[1]	Erosional truncation events
North											
Kalaloch (1)	5277650N395860E	150	Platform/beach	Cobble plume	100	1	Sandy cobble	Sandy cobble	—	CS	2
Whale Creek (2)	5259800N398890E	30	Beach/lagoon	Clastic dike	20	2	Gravelly sand	Sand	Peat	CB	1
North Cove (3)[2]	5175870N419450E	100	Tidal inlet	Lateral spread	50	5	Sand	Sand	Muddy sand	CD,CS,CB	2
Shoal Water (4)[2]	5175500N419910E	100	Estuarine	Clastic dike	20	2	Sand	Muddy sand	—	CB	—
Ramsey Pt. (5)	5168200N429200E	20	Estuarine	Clastic dike	15	2	Sand	Sand	Muddy sand	CS,MF,CB	—
Central											
Netarts Bay (6)	5027420N426800E	50	Estuarine	Clastic dike	20	2	Gravelly sand	Mud	Mud	CS, MF	—
Cape Kiwanda (7)	5008510N423810E	30	Beach/lagoon	Clastic dike	15	1	Sand	Muddy peat	Peat	CS,MF,CB	—
Roads End (8)	4984110N420420E	50	Beach/dune	Clastic dike	10	2	Sand	Sand	—	CS, CB	3
Nelscott Beach (9)	4977010N419300E	20	Dune/pond	Clastic dike	5	1	Sand	Sand	Mud	CS, CB	3
Sea and Sand (10)	4968170N417640E	50	Beach/lagoon	Clastic dike	30	2	Sand	Mud	Peat	CS, CB	1
Otter Rock (11)	4954650N416500E	50	Beach/dune	Clastic dike	20	2	Sand	Sand	—	CS	2
Agate Beach (12)	4946840N416040E	20	Beach/dune	Clastic dike	30	2	Sand	Sand	—	CB	—
Deer Creek (13)[3]	4928650N413180E	30	Platform/lagoon	Flame	30	1	Sandy cobble	Mud	—	BS, MF	—
Seal Rock (14)	4926800N413900E	20	Beach/dune	Clastic sill	25	2	Sand	Sand	—	CB	1
Alsea Bay (15)	4922100N416000E	20	Estuarine	Clastic dike	30	3	Silty sand	Sandy mud	Mud	CS	—
South											
Crown Point (16)[2]	4797810N394870E	10	Beach/?	Dike	30		Sand	Sand	—	CB	—
Winchester (17)[2]	4790200N393400E	20	Beach/?	Dike	15	1	Muddy sand	Sand	—	CS	—
Pony Ridge (18)[2]	4799010N397770E	90	Estuarine	Lateral spread	100	6	Sand	Sand	—	CD,CS,CB	—
Boat House (19)	4800320N392000E	10	Beach/dune	No fluidization	—	—	Sand	Muddy sand	Mud	—	—
Sunset Bay (20)	4798650N388900E	50	Beach/dune	Convolute beds	—	—	Sand	Sand	—	—	—
Merchants (21)	4786580N387000E	100	Dune/pond	Clastic dike	5	1	Sand	Sand	Mud	CB	—
Bandon (22)	4776000N386850E	100	Fluvial/tidal	Clastic sill	10	2	Sand	Gravelly sand	—	CB	1
Floras Lake (23)	4750130N376400E	100	Beach/dune	Clastic dike	25	3	Sand	Gravelly sand	—	CS, CB	2
Cape Blanco (24)	4742350N373780E	50	—	Cobble plume	100	2	Sandy cobble	Sandy cobble	—	CS	—
Paradise (25)	4736410N375760E	100	Beach/dune	Clastic sill	35	2	Gravelly sand	Sand	—	CD, CB	2

[1] CP=cobble plume; LS=lateral spread; CD=clastic dike; CS=clastic sill; BS=basal shear; MF=mud flowage; CB=convolute beds
[2] Older terrace, presumed to equal or exceed 125 ka.
[3] Deposit fill in valley cut of late Pleistocene terrace. Age is younger than terrace.

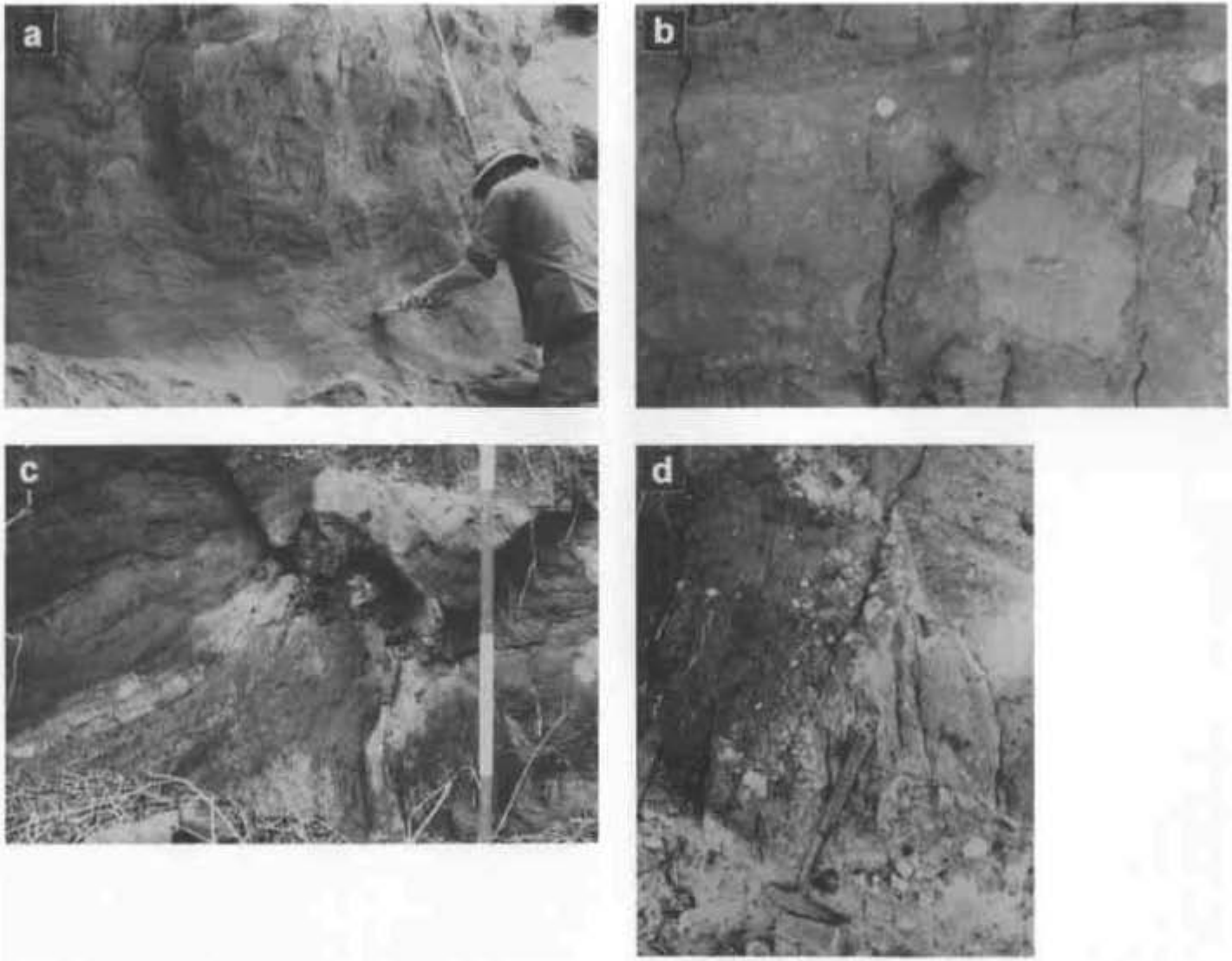

Figure 6. Photographs of (a) highly convoluted beds of beach laminae (originally planar) feeding clastic dikes that terminate in backshore eolian dune deposits, north of Lincoln City (site T8); (b) outcrop exposure showing clastic sills and entrained/dismembered sand blocks developed under a deformed peat, south of Lincoln City (site T10) (U.S. quarter-dollar coin in upper center for scale); (c) large clastic dike deforming originally horizontal beach laminations, north of Newport (site T12) (staff divisions are 30 cm long); (d) basal shear of wave-cut platform developing mudstone breccia and associated breccia/cobble flame structure in overlying lagoonal mud, south of Newport (site T13).

examined from Cape Kiwanda to Seal Rocks. The source beds are well-sorted beach sand (Figure 6a) or mixed sand and gravel (Figure 6b). However, the extension of fluidization features upwards into eolian dunes or lagoonal peats argues against aseismic liquefaction from surf pounding. Two of the localities (sites T8 and T9) might demonstrate three events each of paleoliquefaction: Each disturbed layer displays erosional truncation of fluidization features, such as small dikes, flames, and/or convolute beds (Figure 7). Large clastic sills (greater than 20 cm wide) are locally developed under capping layers of peat (sites T7 and T10) or mud (interdune pond deposits at site T9). Whereas large dikes are observed under a deformed peat layer in a lagoonal setting at site T10 (Figure 6b), only small dikes (5–10 cm in width) cut through the deformed peaty capping layer there.

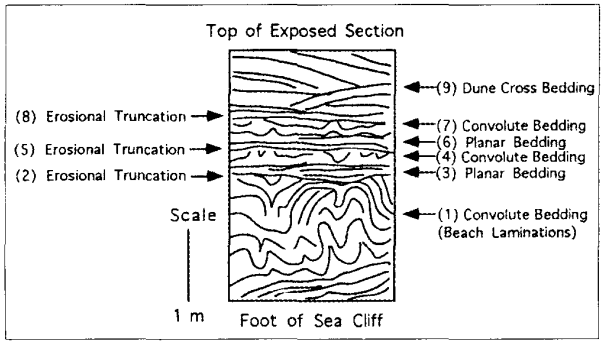

Figure 7. Drawing of episodic paleoliquefaction and erosional truncation sequences at Roads End (site T8). See photograph of lower convolute beds in Figure 6a. The truncation of several convolute beds implies syndepositional paleoliquefaction. Possibly three events of liquefaction and erosional truncation are represented at this site. The youngest flame and convolute beds extend upwards from beach backshore to eolian dune deposits.

Paleoliquefaction sites are also common in the marine terraces north and south of Newport. Liquefaction features include clastic dikes at sites T11 and T12 (Figure 6c) and basal shear structures, such as at site T13 (Figure 6d). In the Newport area, the late Pleistocene wave-cut platform is cut into Tertiary mudstones. Where exposed by local uplift, the weathered platform surface shows unusual evidence of brecciation by mud injection and shear flow. Pieces of the weathered platform (Tertiary mudstones) are entrained into convoluted beds and/or flames. The flames and the convolute bedding are restricted to a couple of meters above the platform (bedrock) contact. Vertical orientations of flames indicate that basal shears are probably not the products of postdepositional landsliding. Clastic dikes are absent from the several observed basal shear sites, but sills are common in adjacent sandy facies. The combination of platform-surface brecciation and fluidization of adjacent sandy facies argues for a cyclic stress mechanism of disturbance at these sites.

A brief survey of marine terraces on the north side of Alsea Bay located a paleoliquefaction site (20-m road-cut exposure) that is dominated by a large clastic sill and dike complex (site T15). Measured sections at this site show an abundance of clastic sills feeding rare dikes (Figure 8). The

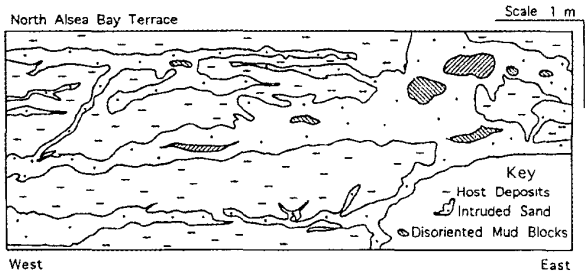

Figure 8. Drawing of large clastic sill and dike complex in tidal-flat deposits from late Pleistocene terrace at Alsea Bay (site T15).

sand-filled sills display sharp (eroded) upper and lower contacts with muddy sand host deposits. The sharp upper contacts were apparently produced by shear-flow erosion of the host deposits during sill injection. The clastic sills also display intruded contacts at their lateral terminations and disoriented (inclined) mud blocks surrounded by structureless matrix or horizontal shear bedding within the sill interiors. Whereas some of these clastic sills might represent minor fluidization of preexisting beds, other sills show evidence of substantial shear flow including eroded contacts, internal flow banding and transport of exotic mud blocks. The extensive fluidization of these shallow tidal-flat deposits is interpreted to represent (1) long duration of coseismic liquefaction and/or (2) multiple liquefaction events.

Coos Bay to Cape Blanco (Figure 4c)

The southern study area contains highly deformed marine terraces, an indication of its proximity to the accretionary wedge fold and thrust belt (Peterson and others, 1991a). Marine terrace outcrops were examined along an east-west traverse from the south end of Coos Bay to the coast. Sites T16 and T17 are from the Metcalf terrace (>125 Ka) that was disrupted by late Quaternary faulting (Madin and others, 1995). These two localities include clastic dikes, 30–50 cm in width at Crown Point (site T16) and 15 cm in width at Winchester (site T17). Large convolute beds and flames are associated with the fluidized beds at the Crown Point site (Figure 9a). The host deposits at sites T16 and T17 are thought to be beach sand, but the terrace deposit thickness (20–40 m) implies more complex shoreface settings. Very large dikes and lateral spreads are also found in a road-cut exposure of an older deposit at the top of Pony Ridge (site T18 and Figure 9b). The age of this unit has not been established, but the relatively minor amount of interstratal weathering implies a Quaternary age. Little primary structure is left at the Pony Ridge locality, where the host deposits are intruded by numerous dikes, sills, and convolute bedding along a 90-m road-cut exposure.

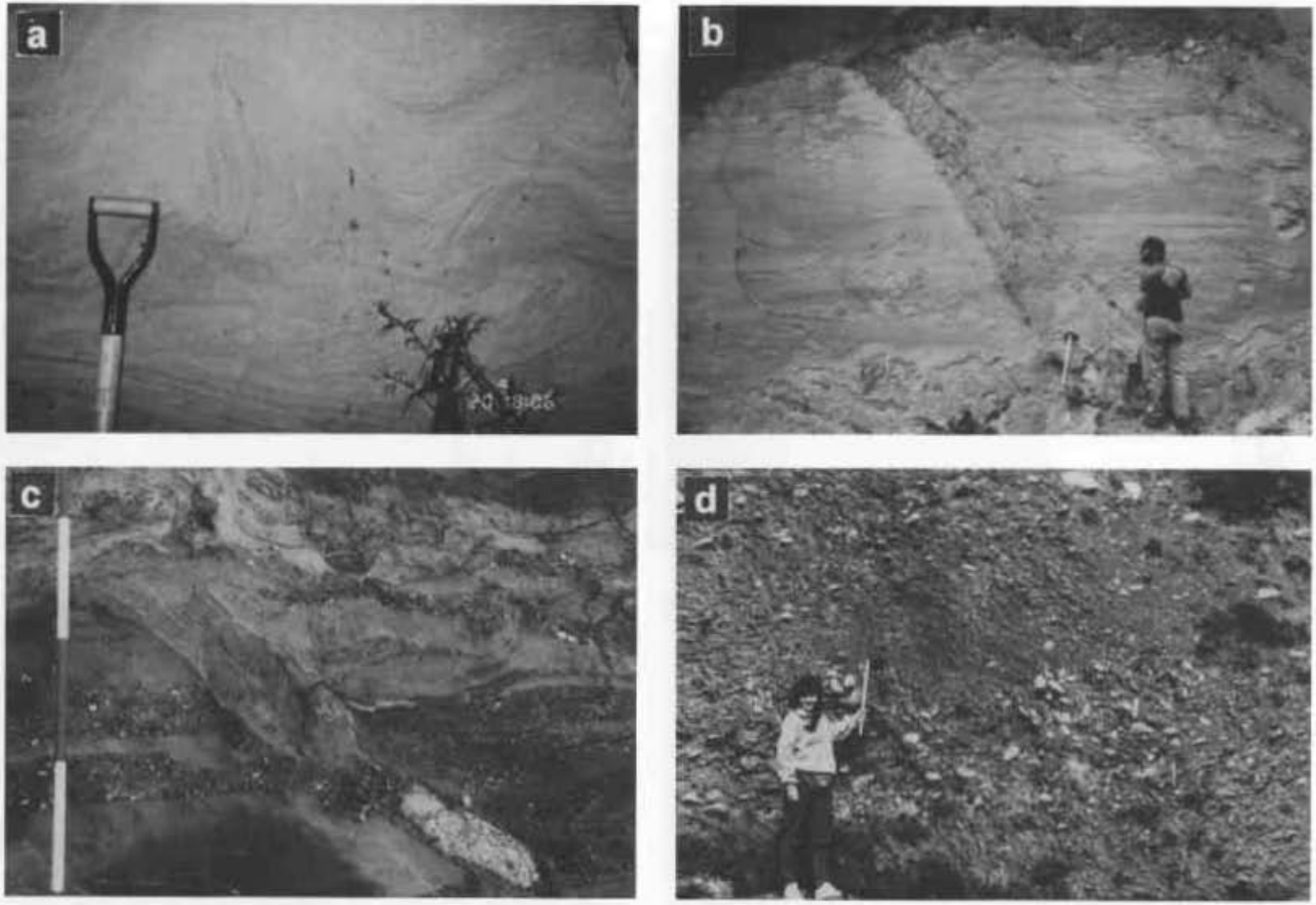

Figure 9. Photographs of (a) convolute beds of deformed beach laminations in Metcalf terrace near Crown Point (site T16) (a large clastic dike at least 30 cm wide was found nearby in the Crown Point road-cut exposure); (b) lateral spread, dikes, and sills at Pony Ridge (site T18); (c) clastic dike and sills cutting sand and gravel layers in beach backshore deposit at Floras Lake (site T23), with diatomaceous mudstone (white elongate feature at lower right) lodged in sill-dike juncture (staff divisions are 30 cm long); (d) large cobble plumes at Cape Blanco (site T24).

Several other localities (sites T19–T22) were examined between Coos Bay and Bandon due to their proximity to reported Quaternary faults or folds along this coast. For example, Merchants Beach (site T21) sits on the west flank of the uplifting Cape Arago (Pioneer) anticline. Quaternary faults are reported for the Boat House (site T19), Sunset Bay (site T20), and Bandon (site T22) localities (Madin and others, 1995; Goldfinger and others, 1992; Geomatrix Consultants, Inc., 1995). The well-exposed deposits of the Whisky Run and Pioneer terraces, 80 and 105 Ka respectively, at these localities (McInelly and Kelsey, 1990) show only weak to moderate evidence of fluidization. Thin source beds (site T20), eolian dune host deposits (site T21), and gravelly sand host deposits (site T22) might account for the weak fluidization at these localities. However, similar depositional settings in the central study area (sites T6–T15) yield equivalent or better paleoliquefaction evidence.

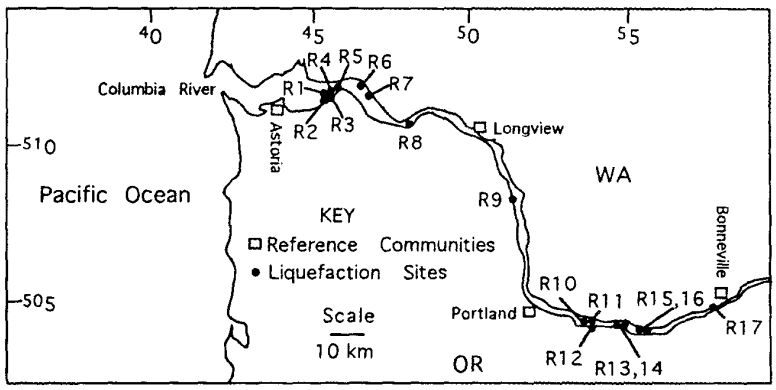

Figure 10. Map of late Holocene paleoliquefaction sites (R1–R17) in the Columbia River islands between Astoria and Bonneville.

A young terrace locality that does include large fluidization features in a beach-dune setting occurs just south of Floras Lake on the north side of Cape Blanco (site T23). Clastic dikes and sills up to 25 cm and 50 cm wide, respectively, are abundant in this 100-m sea-cliff exposure (Figure 9c). Two sets of erosionally truncated convolute beds indicate that, at this locality, multiple liquefaction events occurred syndepositionally, i.e., within the period of marine highstand.

At Cape Blanco (site T24), a terrace deposit exposed in ravine and beach cliffs contains poorly organized cobble plumes (Figure 9d). Though not as well imbricated as those at Point Brown, Washington (site T1), the apparent convection plumes at Cape Blanco are larger, reaching 2 m in width. Another cobble liquefaction site (not included in Figure 4 or Table 1) exists in a terrace deposit located about 1 km northwest of the Elk River mouth (UTM 4739300N-375600E). Fluidization of underlying sand deposits might have disrupted the overlying cobble beds at this site. South of the Elk River mouth, several paleoliquefaction localities are exposed in the beach cliff. At one locality (T25), large clastic sills (35 cm wide) and small dikes entrain pea gravel into hosting dune deposits. The fluidization features abruptly decrease in abundance and scale several meters above the transition between beach backshore and eolian dune facies. Erosional truncations of convolute beds at this locality indicate that the paleoliquefaction events were syndepositional with the marine highstand deposition.

LATE HOLOCENE PALEOLIQUEFACTION IN THE COLUMBIA RIVER

Lower river valley

Clastic dikes are exposed in shallow cutbanks and wave-cut benches of many islands in the lower reaches of the Columbia River. Island outcrops surveyed in 1992 and 1993 include Marsh, Karlson, Brush, Woody, Price, Hunting, Wallace, and Deer Islands, among others (sites R1–R17, Figure 10; data summary in Table 2). The observed clastic dikes range in width from 30 cm at site R1 (Figure 11a) to only 3 cm at adjacent locality R2. The sand-filled dikes cut capping mud layers about 1 m thick but generally terminate in peaty deposits or erosional surfaces 0.5–1 m below the modern floodplain (see "Paleoliquefaction chronostratigraphy" below). Accretionary-bank sand deposits under the capping mud layers (Peterson and others, 1994) are the likely source beds for the clastic dikes. Cementation along the dike walls produces erosionally resistant selvages that stand out from the wave-cut benches, observable at low tides at site R8 (Figure 11b).

Vibracores driven to subsurface depths of 5–6 m at several positions at sites R1, R6, R7 (Figure 11c), and R8 demonstrate abundant subsurface evidence of clastic dikes and other intruded structures. The 30-cm-wide dike at Marsh Island (site R1) was followed to a depth of 2.5 m before it angled away from paired vibacores. Fluidization features recovered in vibracores (Figure 11d) occur to depths of at least 6 m below corresponding venting surfaces at sites R1, R7, and R8 (Craig and others, 1993). Anomalous core sections (20–100 cm thick) that lack any primary bedding occur at various depths in most of the recovered vibracores (see, e.g., Figure 12). These sections might represent fluidized source beds or clastic sills, as evidenced by (1) intruded contacts, (2) entrained (disoriented) mud clasts, and/or (3) zones of disturbed or absent cross-bedding that are seen in the vibracores. Undisturbed cross-bedding seen in adjacent core sections implies that the vibracoring itself was not the cause of fluidization. More importantly, iron oxide stains along deep intruded contacts (4–6 m depth) indicate that the (possibly several) fluidization events clearly predate the vibracoring.

Summaries of vibracore logs and supporting geotechnical data from the lower Columbia River islands are in preparation (B. Atwater, personal communication, 1995).

Figure 11. Photographs of (a) large sand-filled clastic dike (30 cm wide) cutting mud-cap layer at Marsh Island (site R1); (b) clastic dike cutting mud-cap layer in wave-cut bench at Wallace Island (site R8) (pocket knife for scale at left of dike is 10 cm long); (c) vibracore rig at Hunting Island (site R7); (d) clastic dike in vibracore (V15) at site R7, taken 1 m west of north-south striking dike (20° dip west), section showing breached mud layer, intruded contacts, disoriented mud blocks in sand matrix, and lack of primary cross-bedding in sand.

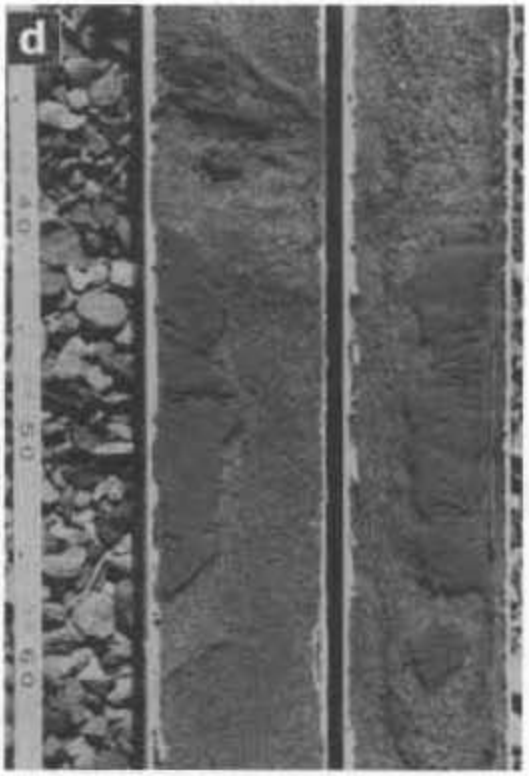

Table 2. Paleoliquefaction localities in exposed cutbanks of Columbia River islands (shown in Figure 10)

Site name (number R-)	UTM coordinates	Exposure length (m)	Dike width (cm)	Sill width (cm)	Source bed lithology	Source bed depth (m)	Host deposit lithology	Capping bed lithology	Capping bed thickness (m)
Western islands									
Marsh Is. (1)	5119080N454000E	100	30	20[1]	Sand	>2.5	Mud	Mud	1
Karlson Is. (2)	5116410N454600E	30	3	—	Sand	>1	Mud	Mud	2
Blind Slough (3)	5116440N456210E	50	0	0	—	—	—	Mud	>3
Brush Is. (4)	5119710N454370E	50	15	—	Sand	>1	Mud	Mud	1
Woody Island (5)	5121450N457650E	50	15	—	Sand	>1	Mud	Mud	1
Price Is. (6)	5122490N465660E	100	7	—	Sand	>1.5	Mud	Mud	1.5
Hunting Is. (7)	5119120N467670E	200	15	20[1]	Sand	>1.5	Mud	Mud	1.5
Wallace Is. (8)	5109700N479100E	100	8	—	Sand	>1.5	Mud	Mud	1.5
Deer Is. (9)[2]	5092100N511900E	1,000	10	—	Sand	1.0–3.0	Mud	Mud	1.0–3.0
Eastern islands									
Government Is. (10)	5045900N540550E	50	0	5	—	—	—	Mud	>3
N. McGuire Is. (11)	5045650N540920E	50	1	3	Sand	>1.5	Sandy mud	Mud	>2
S. McGuire Is. (12)	5045350N541300E	50	6	20	Sand	>1	Sandy mud	Mud	2
W. Sandy Delta (13)	5045600N547000E	30	5	15	Sand	>1.5	Sandy mud	Mud	2
E. Sandy Delta (14)	5046000N547600E	30	3	15	Gravelly sand	2	Muddy sand	Mud	3
W. Reed Is. (15)	5044150N553350E	50	6	10	Sand	>1.5	Muddy sand	Mud	2
E. Reed Is. (16)	5044100N555470E	30	3	5	Sand	1	Mud	Mud	2
Pierce Is. (17)	5052100N577000E	30	5	13	Sand	1	Muddy sand	—	1

[1] Sill width data from vibracore.
[2] Deer Island dike width data from L. Palmer (pers. comm., 1996), limiting radiocarbon age <690±70 RCYBP (Obermeier, 1995).

Upper river valley

Cutbanks in McGuire, Reed, and Pierce Islands and the Sandy River delta of the upper Columbia River valley (sites R11–R17, Figure 10 and Table 2) contain small clastic dikes and sills beneath thick capping mud layers. Maximum dike widths are on the order of 5–6 cm. The more abundant sills reach 15–20 cm in thickness. At the Sandy River delta (site R13), fluidized source beds (Figure 13a) feed thin clastic dikes (2–5 cm in thickness) that penetrate about 2 m into overlying sandy mud. Fluidization features terminate at least 0.5 m below the modern island surface. No dikes were found along the south side of Government Island (site R10), where only mud is exposed in a 3-m-high outcrop. However, clastic sills (5 cm wide) are observed low in the exposed section, presumably near the bottom of the mud cap. In 50 m of outcrop exposed along the south side of Reed Island (site R15), clastic sills outnumbered dikes by more than 20:1 (Figure 13b). Coarse sand in the sills must have risen via clastic dikes from coarse channel deposits below the exposed host deposits of fine sand and overlying flood silts. Clastic sills also predominate in the exposed cutbank section at Pierce Island (site R17), although some short dikes interconnect sills between muddy sand layers there (Figures 13c,d).

Some effort was made to establish whether more than one event of fluidization was apparent in the exposed cutbanks of the islands in the upper river valley. These preliminary efforts were unsuccessful. Small dikes were observed to cut clastic sills at sites R13 and R15, but a lack of weathering or cementation precludes a determination of the age relations of the sills and dikes. No subsurface vibracoring has been performed in those islands, so the potential depth of paleoliquefaction evidence there is not known. Finally, some of the sills in these islands might have formed via in situ liquefaction of preexisting sand layers rather than by intrusion of clastic sills from feeder dikes. The thickness of these sills might not reflect intensity of liquefaction, but rather the incipient fluidization of layered source beds. For this reason, the thickness of the clastic sills is not used to compare potential strength of shaking between the Columbia River paleoliquefaction sites.

Paleoliquefaction chronostratigraphy

The timing and correlation of the most recent paleoliquefaction event(s) in the late Holocene deposits of the Columbia River were addressed by several independent methods. These methods include stratigraphic correlation with regional coseismic subsidence (lower river valley), radiocarbon dating and tephrachronology (lower and upper river valley), and observations of surficial "historic" deposits (upper river valley).

In the lower river valley localities (sites R1, R6, and R7),

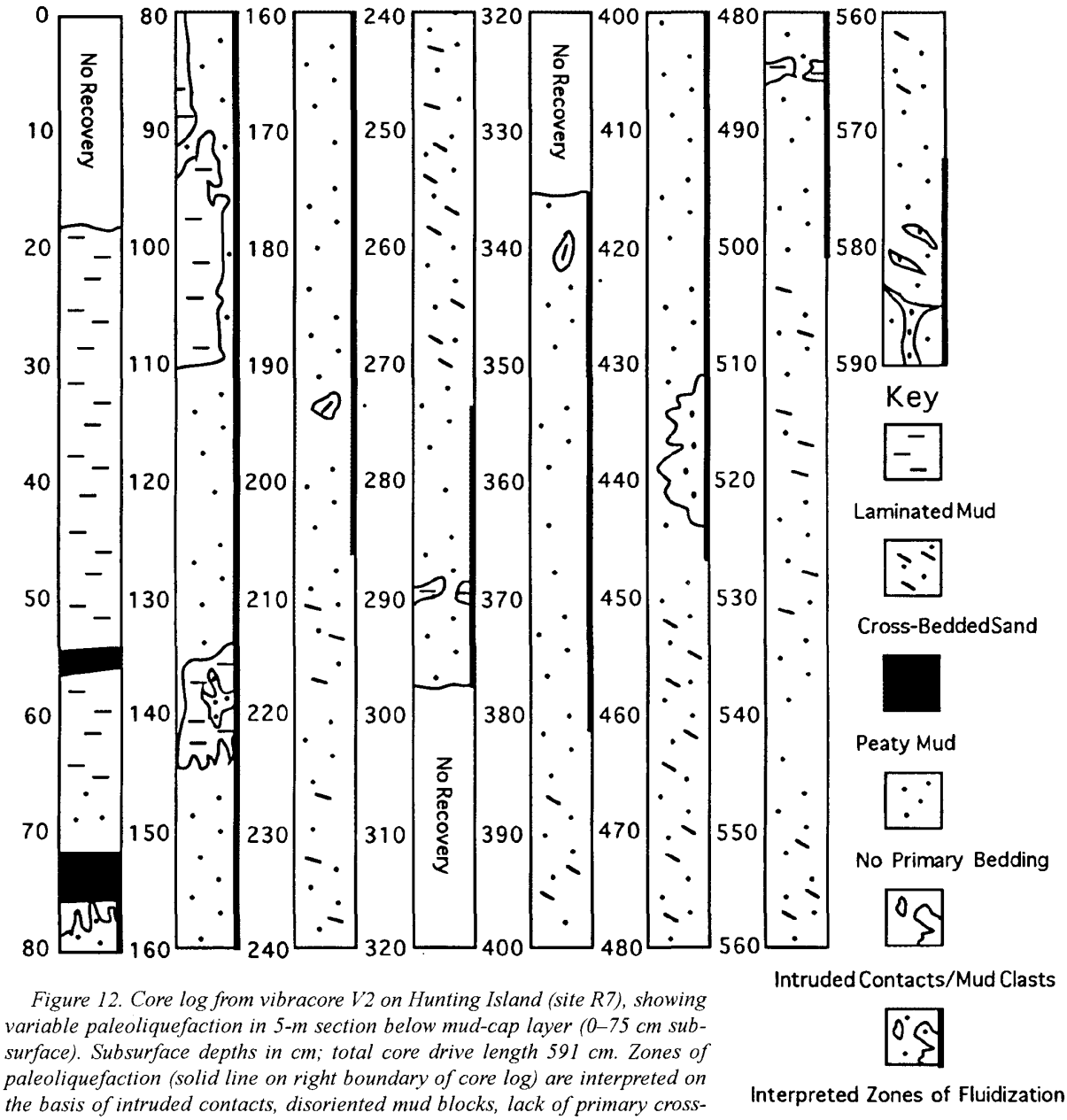

Figure 12. Core log from vibracore V2 on Hunting Island (site R7), showing variable paleoliquefaction in 5-m section below mud-cap layer (0–75 cm subsurface). Subsurface depths in cm; total core drive length 591 cm. Zones of paleoliquefaction (solid line on right boundary of core log) are interpreted on the basis of intruded contacts, disoriented mud blocks, lack of primary cross-bedding, and/or pseudo-shear bedding parallel to injected clastic flow.

thin sand layers (1–3 cm thick) are infrequently preserved immediately above buried wetlands. These features are interpreted to represent fluidized sand that was vented onto the preexisting wetland surfaces (Obermeier, 1995). However, the first correlation of paleoliquefaction and coseismic subsidence in the lower Columbia River was made at Karlson Island (site R2). At this site, muddy flowage disrupted a buried peat surface that was also intruded by small clastic dikes and sills (Figure 14a). The small sand dikes terminated at the top of the disrupted peat layer which was itself overlain by undisturbed (horizontal) mud laminations.

The disrupted peat layer at Karlson Island was traced across the channel to cutbank outcrops in Blind Slough (site R3). There, in situ spruce roots in the buried peaty horizon were sampled for radiocarbon dating. The spruce roots had a limiting (conservatively old) age of 700±60 RCYBP ±1σ (Beta Analytic, Inc., sample no. 56407). The last two regional events of coseismic subsidence in the lower Columbia River valley area occurred at about 300 and 1,100 yr B.P. (Atwater, 1987; Darienzo, 1991). Therefore, the paleoliquefaction was tentatively attributed to the last Cascadia earthquake about 300 yr ago. Subsequent radio-

carbon dating of buried soils and tree-ring counts from submergence-killed trees in the lower Columbia River islands (Atwater, 1994) confirm that the most recent event of paleosubsidence in the lower Columbia River does correlate to the A.D. 1700 Cascadia earthquake.

The amount of coseismic paleosubsidence diminishes upriver, until it becomes undetectable between Hunting and Wallace Islands. However, an independent time line (tephra layer) was found about 0.5 m below the buried wetland horizon at Marsh Island (Figure 14b). A gray silt layer (1–3 cm thick) is locally present some 5–20 cm below the tephra layer. The tan-colored tephra layer was subsequently traced to Hunting and Wallace Islands, where it is also cut by shallow clastic dikes. Petrographic analysis confirms an abundance of ash shards (30–90 percent of silt-sized grains) in the tephra layer. Instrumental neutron activation analysis (INAA) of pumice fragments from the Marsh Island tephra layer (Table 3) discriminates the volcanic source, i.e., Mount St. Helens, from other potential sources, e.g., Mount Mazama and Glacier Peak (Figure 15) (Gates, 1994). The relative age of this tephra layer (greater than 300 yr B.P.) and the extent of its distribution (volume) in the preserved deposits of the lower Columbia River indicate an origin from the Mount St. Helens set W eruptions at about A.D. 1480 (Yamaguchi, 1985; Mullineaux, 1986).

Table 3. *INAA geochemical data for pumice fragments from Marsh Island tephra layer*

	Pumice sample NG–10		Pumice sample NG–11	
Element	Concentration (ppm)	Uncertainty (percent)	Concentration (ppm)	Uncertainty (percent)
As	6	36.8	3	34.2
Rb	55	10.9	61	10.7
Cs	2.1	5.5	2.4	6.2
Sr	377	12.3	326	14.6
Ba	432	5.7	474	5.4
Sc	6.1	1	6	1.2
Cr	17	6.8	17	6.2
Fe (%)	2.1%	1.1	2.1%	0.9
Co	5	4.7	4.9	4.6
Zn	41	30.5	44	27.3
Ce	34	2.1	35	2
Nd	21	14	17	38.8
Sm	3.6	5.6	3.3	6.1
Eu	0.9	4.4	1	ND
Yb	2	11.7	2	12.9
Lu	0.2	9.7	0.2	9.5
Zr	127	39.1	139	31.7
Hf	4.4	4.2	4.3	5.5
Ta	1.1	17.4	1.5	17.2
Th	6.3	3.2	7.6	2.5
La	29	6	34	3.7

In the upper river valley, the apparent "tephra" layer(s) exposed in cutbanks of McGuire and Reed Islands and the Sandy River delta are locally cut by small clastic dikes. Petrographic analysis of the anomalous pink layers (1–3 in number) shows them to be enriched in altered rock fragments and hypersthene, but ash shards are rare. INAA geochemical analysis of the target layers at Reed Island shows the layers (3–10 cm thick) to be largely diluted by Columbia River sediments (Barnes, 1995). A charcoal sample in contact with the pink "tephra" layer from the west cutbank of the Sandy River delta (Figure 16a) has a radiocarbon age of 410±70 RCYBP ±1σ (Beta Analytic, Inc., sample no. 67448). On the basis of this radiocarbon date and the widespread occurrence of these anomalous "tephra" layers in the upper river islands, we ascribe their origin to the Mount St. Helens set W eruptions. Confirmation of this source awaits sampling and geochemical analysis of possible ash shards or pumice fragments from the target "tephra" layers.

Anomalous beds of coarse gray sand are also exposed in the Sandy River delta cutbanks, which are dominated by Columbia River sand. At several meters' depth, these coarse gray sands are cut by the clastic sills and dikes; however, similar gray sands in isolated scour fills near the top of the section are undisturbed. These coarse gray sands might represent Mount Hood lahars or reworked lithic-rich sand carried down the Sandy River during floods. One set of lahars apparently caused foundering of the local overburden and liquefaction in Columbia River flood silts immediately downriver from the Sandy River delta (Vockler and others, 1994). However, no such evidence was observed in the Sandy River delta cutbanks (sites R13 and R14). In any case, the Sandy River lahars cannot account for the paleoliquefaction at McGuire (sites R11, R12), Reed (sites R15, R16), and Pierce Islands (site R17), well away from the Sandy River confluence with the Columbia River.

Two age-limiting radiocarbon samples were collected at the uppermost reach of intruded sands at the Sandy River delta (R13) and Pierce Island (R17) sites. Wood fragments from these two localities (Figure 16) have radiocarbon ages of 250±70 RCYBP ±1σ (Beta Analytic, Inc., sample no. 67446) and 260±50 RCYBP ±1σ (USGS-WW540 Livermore-CAMS-22498), respectively. These radiocarbon ages confirm broader field observations (below) indicating that the paleoliquefaction event(s) are of latest prehistoric age. A total of about 1 km of well-exposed outcrop was examined from the Government, McGuire, Sandy River, Reed, and Pierce Island cutbanks. None of the examined sections showed evidence of intruded sands reaching modern floodplain deposits, i.e., the upper 20–30 cm of exposed sections. Fluidization was also absent in cross-bedded sands filling shallow scours at the top of the exposed sections at several of these localities. Apparently, the Vanport flood of 1948, the Olympia earthquakes of 1949 and 1965, and the Portland-Vancouver earthquake of 1962 were insufficient to produce liquefaction at any of the observed cutbank localities (sites R10–R17) in the Columbia River islands east of Portland.

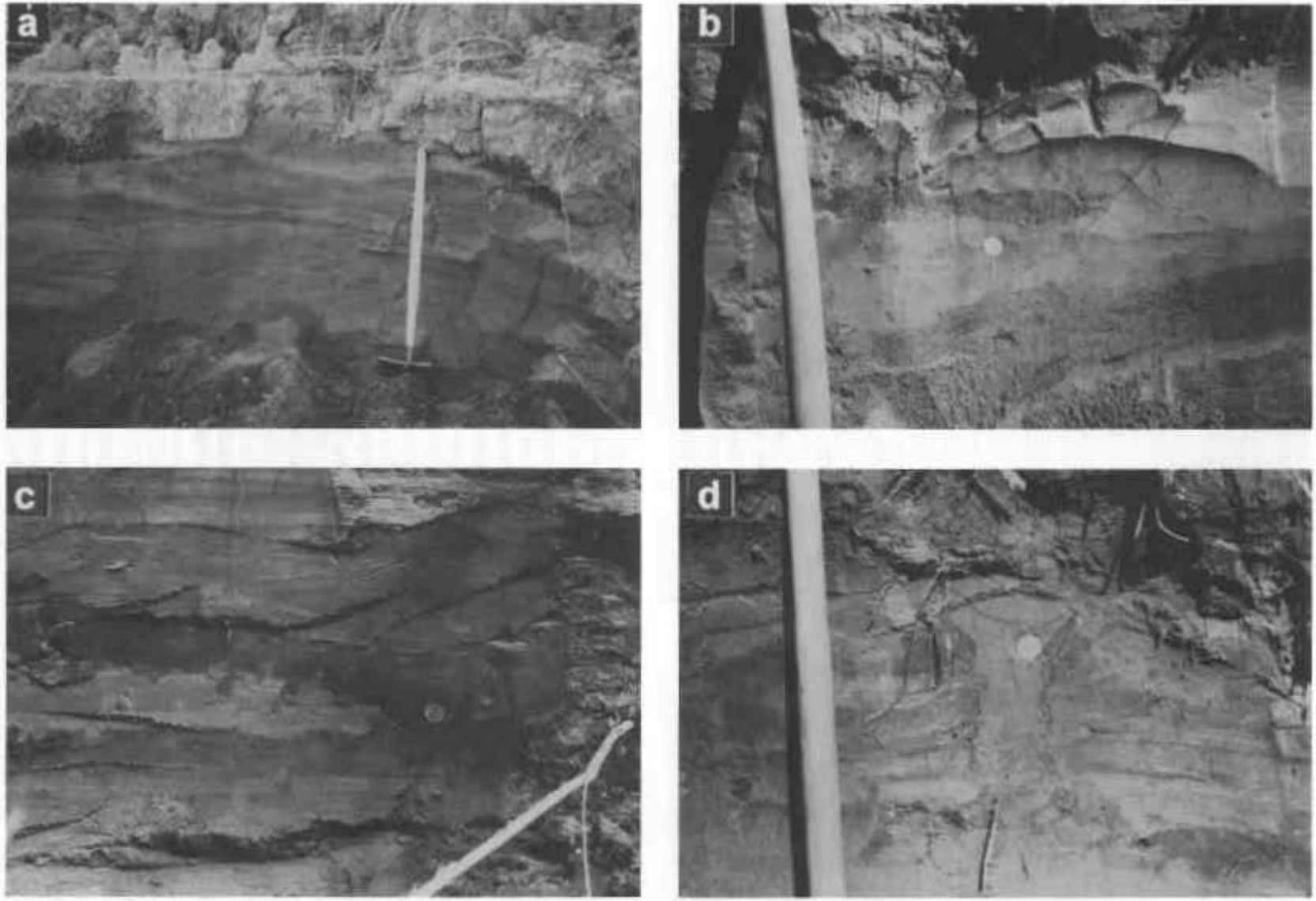

Figure 13. Photographs of (a) interfingering intruded sills in or near source beds (sand) at Sandy River delta (site R13) (hoe handle 40 cm long); (b) coarse sand in clastic sills injected into fine-sand host deposits at Reed Island (site R15); (c) clastic sills injected into muddy sand host deposits at Pierce Island (site R17); and (d) clastic dike, 5 cm wide, connecting clastic sills at Pierce Island (site R17). Quarter coins for scale in Photographs b, c, d.

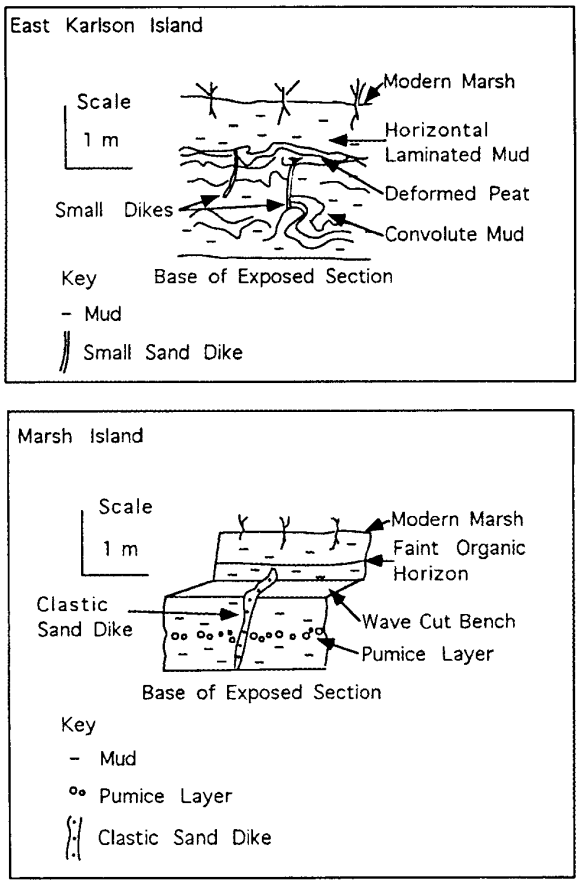

Figure 14. Drawings of exposed cutbank sections from (a) Karlson Island (site R2) and (b) Marsh Island (site R1) in the lower Columbia River valley. The Karlson Island section shows convolute mud beds and small clastic dikes associated with a deformed buried-wetland soil. Horizontally laminated mud above the deformed wetland soil is undisturbed, thereby linking the paleoliquefaction (sand intrusion) and paleosubsidence. The paleosubsidence is traced regionally to the last Cascadia earthquake about 300 yr ago (Atwater, 1987; Darienzo, 1991). The Marsh Island section shows a large clastic dike cutting a tephra layer that contains abundant ash shards and small pumice blocks.

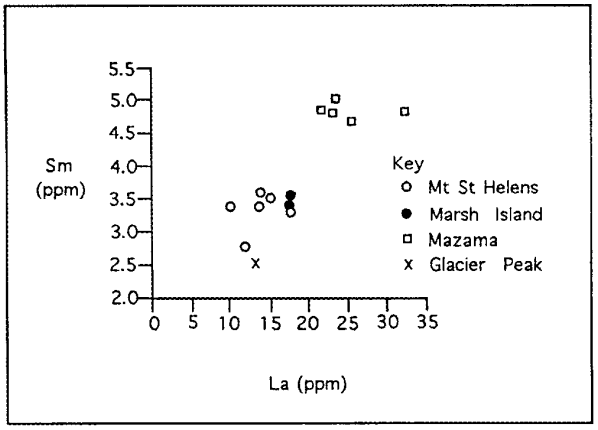

Figure 15. Plot of INAA rare-earth concentrations (Sm=samarium, La=lanthanum) for Marsh Island tephra pumice blocks (solid circles) and other potential tephra sources, including Mazama eruption (open squares), Mount St. Helens eruptions (open circles), and Glacier Peak eruption (x). The Marsh Island tephra geochemistry (Table 3) correlates with the Mount St. Helens source. It is also distinguished from the Mazama and Glacier Peak sources on the basis of Sm/Ce ratios and La/Ce ratios, among others. The data for the Mazama, Mount St. Helens, and Glacier Peak eruptions are taken from a compilation by Gates (1994).

DISCUSSION

Distribution of late Pleistocene evidence of paleoliquefaction

We assume that cobble plumes, basal shears, and lateral spreads are evidence for probable strong shaking in settings where aseismic paleoliquefaction is unlikely. A regional plot of these features (Figure 17) shows them to be uncommon (present at 5 out of 25 reported sites) but widespread across the Washington, central Oregon, and southern Oregon study areas. Clastic dikes of at least 5-cm width are more common (observed in 15 of 25 reported sites). They provide a different indicator for comparing probable response to coseismic liquefaction between the three study areas. Specifically, maximum dike width is assumed to reflect strength of shaking, assuming all other variables to be constant (Obermeier, 1996). Large lateral spreads (i.e., vertical fissures at least 50 cm wide) are possibly related to slope failures and thus are not included in this semiquantitative analysis of moderate-size dikes (5–49 cm wide). Regional plots of maximum dike width in the Pleistocene coastal terraces show a relatively uniform distribution of maximum dike widths along the margin (Figure 17). Within the limit of the coastal terrace positions, there is no apparent correlation between dike size and distance from the trench.

The presumed active structures, i.e., mapped Quaternary surface faults and folds in the southern Oregon study area, yield conflicting evidence of paleoliquefaction. For example, sites T16 and T18 near Coos Bay contain large-scale fluidization features, whereas sites T19–22 in the Cape Arago area do not (Table 1). Long recurrence intervals between ruptures of these upper plate structures might account for the weak paleoliquefaction evidence observed in their immediate vicinities. If that is true, then regional subduction-zone seismicity might dominate the geologic record of coseismic liquefaction. Unfortunately, the question of local versus regional coastal seismicity is left unresolved for the late Pleistocene marine terraces. However, the preliminary evidence of probable coseismic fluidization

Figure 16. Drawings of exposed cutbank sections from west Sandy River delta (site R13) and Pierce Island (site R17) in the Columbia River valley east of Portland. The south end of the Sandy River delta section contains a pink "tephra" layer that is cut by small clastic dikes. A charcoal sample in contact with the pink layer has a radiocarbon age of 410±70 RCYBP. At the north end of the Sandy River delta section, a wood fragment was collected from the maximum height of dike intrusion. The wood fragment has a radiocarbon age of 250±70 RCYBP. The clastic sills at the bottom of the Sandy River delta north section are shown in Figure 13a. The Pierce Island section includes a radiocarbon age (260±50 RCYBP) on a detrital wood fragment from the top of the intruded sands. Small clastic sills and dikes at the lower left and right, respectively, of the Pierce Island section are shown in Figures 13c and 13d.

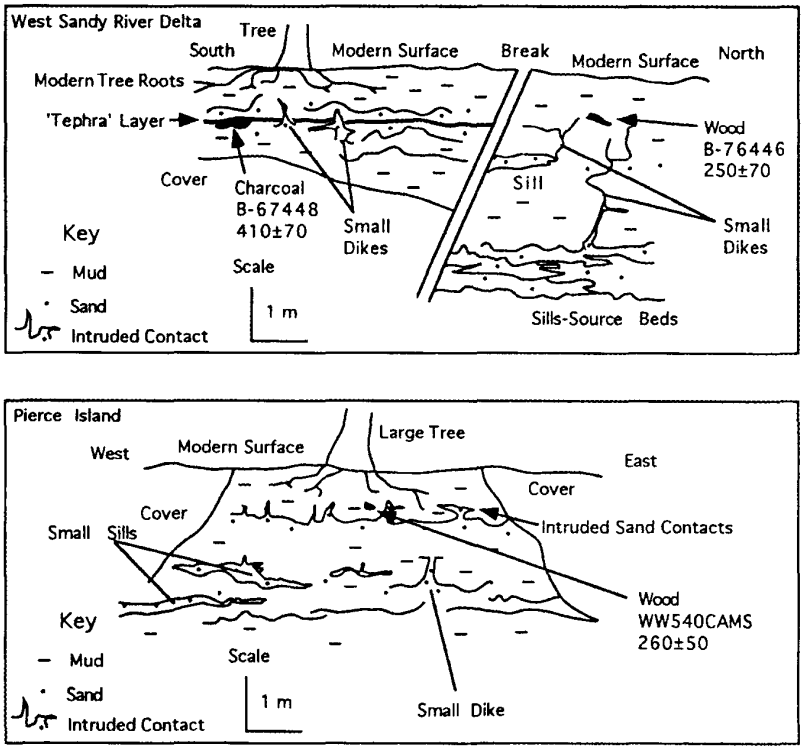

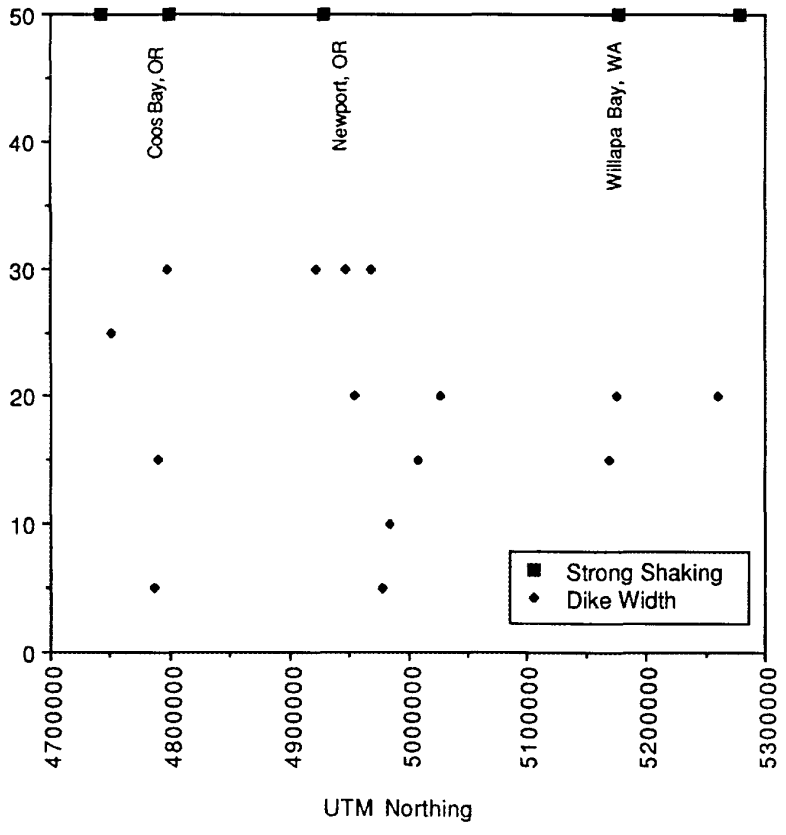

Figure 17. Plot of probable coseismic-fluidization features in late Pleistocene marine terrace deposits (represented as maximum dike widths) as a function of north-south position (UTM coordinates) along the coast. Features interpreted to indicate strong shaking, such as disrupted cobble beds, sheared wave-cut platform surfaces, and lateral spreads, are shown by solid squares for five sites (top of plot). Maximum clastic dike widths between 5 and 30 cm (solid diamonds) are shown for 15 terrace sites.

in the marine terraces of the central Cascadia margin (Peterson and Madin, 1992) is now verified in at least two dozen localities. That is to say that paleoliquefaction evidence of probable seismic origin is widespread in late Pleistocene terrace deposits of coastal Oregon and Washington.

Depositional settings of fluidization features

The largest dikes and lateral spreads in the late Pleistocene deposits are generally found in bay, lagoonal, or thick shoreface settings (sites T3, T10, T15, T16, and T18; Table 1). These settings contain substantial subaqueous sand deposits (5–10 m in thickness), which likely serve as source beds for the larger fluidization features. By comparison, dikes and sills originating in beach backshore settings (sites T8, T9, T11, T21, T23, and T25) rapidly decrease in size and abundance with penetration into overlying eolian dune sand. These relations might reflect dissipation of fluid pore pressure in unsaturated dune deposits. Within the eolian dune facies, the fluidization evidence is often concentrated under low-permeability mud layers, where pore pressures might be locally enhanced. Boundary effects are also apparent in deposits above wave-cut platforms (sites T1 and T14), where cobble plumes, basal shears, and flames are locally concentrated near the platform contacts. Different ground-motion responses between the platform "bedrock" and the overlying unconsolidated deposits might amplify shear stresses near these platform contacts.

In summary, the distribution of observed paleoliquefaction sites within the three study areas of the central Cascadia margin appears to be largely dependent on the presence of exposed deposits that were conducive to cyclic-stress fluidization. The apparent distribution of such deposits is limited by (1) local depositional settings, e.g., facies and groundwater saturation conditions, (2) postdepositional preservation, and (3) modern exposure in cliffs and road cuts. Although liquefaction-susceptible settings are not abundant in the study areas surveyed, they can be found by focused searches of the remnant marine terraces.

Timing of late Pleistocene paleoliquefaction

The relative timing of late Pleistocene paleoliquefaction is constrained at 11 localities by evidence of erosional truncation and subsequent burial of fluidization features. These localities include sites T1–T3, T8–T11, T14, T22–T23, and T25 (Table 1). The probable coseismic liquefaction at these sites was syndepositional with the development of the sedimentary packages above the wave-cut platforms. Vertical upward successions of estuarine, beach, dune, and interdune-pond facies demonstrate that these marine terrace deposits represent transgressive system tracts (TST) or highstand tracts (HST). At least seven of the late Pleistocene sites possibly record multiple events (two or three) of paleoliquefaction, i.e., vertical successions of erosionally truncated and buried fluidization features. The interpretation of multiple liquefaction events is tentative, and further field work to test this hypothesis is warranted.

On the basis of eustatic sea-level records (Pirazzoli, 1993) and the thickness of the late Pleistocene TST-HST sections (typically 3–8 m in height), the periods of depositional record are probably limited to several thousand years each for the 80-, 105-, and 120-Ka terraces. The multiple events of paleoliquefaction possibly recorded at some of the late Pleistocene sites could indicate two or more earthquakes during the several thousand years of record for each locality. Other evidence of multiple earthquakes during the late Pleistocene TST periods is recorded in northern Oregon marine terraces by vertical sequences of episodic peat burial (Mulder, 1992). These episodes of abrupt wetland subsidence in late Pleistocene time have yet to be directly tied to evidence of sand venting. However, muddy flow features and small dikes are associated with disrupted peaty horizons at two sites (T6 and T7) in the northern Oregon study area (Table 1). Better exposures of the disrupted buried peaty units in the late Pleistocene terraces might reveal sand-vented deposits at the buried peat contacts, thus constraining interpretations of seismic source, as discussed below.

Paleoliquefaction evidence of the A.D. 1700 Cascadia earthquake

The most recent episode of paleoliquefaction in the lower Columbia River valley is directly tied to the last CSZ earthquake through correlation of sand venting with regional coastal subsidence (Obermeier, 1995). The buried-wetland evidence of regional subsidence has not been found upriver (east) of Hunting Island. By comparison, evidence of late prehistoric liquefaction is traced up the Columbia River valley through a series of cutbank localities including sites R10–R17 (Figure 10). Paleoliquefaction at these localities is tentatively correlated to the A.D. 1700 event through (1) generally decreasing maximum size and abundance of fluidization features with increasing distance inland, (2) upper bounding radiocarbon dates at two localities (sites R13 and R17), and (3) lower bounding "tephra" layers cut by clastic dikes and sills at four localities (sites R7, R8, R13, and R15).

Maximum dike widths generally decrease from the lower to the upper river valley (Figure 18). However, strong trends in dike abundance and width also occur over much smaller traverses, i.e., normal to the river valley axis. For example, the maximum dike width in the lower river valley decreases from 30 cm (site R1) to 3 cm (site R2) to zero (no dikes) at Blind Slough (site R3), a distance of only 2.5 km. In the upper river valley, the small dikes at McGuire Island (sites R11 and R12) were not observed at nearby Government Island (site R10). The decreases in dike abundance and maximum width at these two traverses might correspond to increases in thickness of the capping mud layer (Table 2). Other factors not addressed here must account for the observed dike variability within individual outcrops of constant capping-layer thickness (B. Atwater, personal communication, 1995).

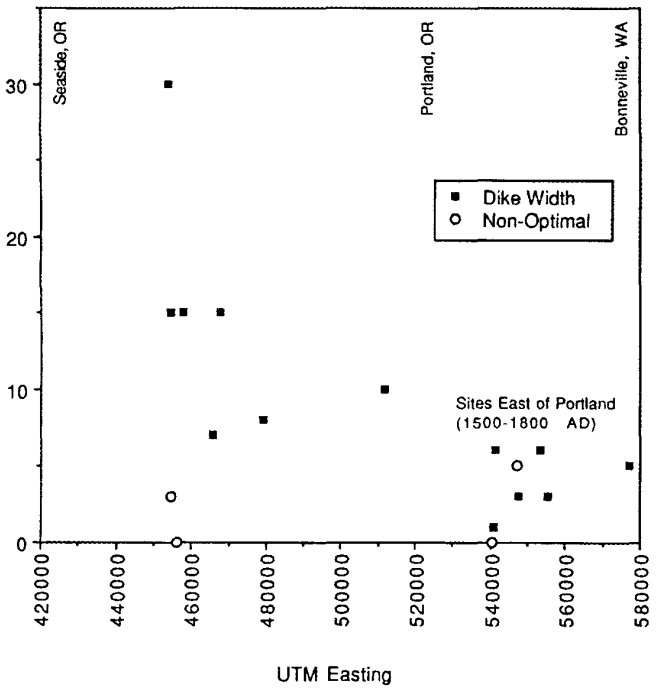

Figure 18. Plot of maximum dike widths in Columbia River island cutbanks as function of position west-east (UTM coordinates) along the Columbia River valley. Cutbanks from optimal sites (shorelines presently adjacent to major river channels) are shown by solid squares. Non-optimal cutbank sites from island interiors that are distal to major river channels are shown by open circles. Measured dikes from the lower Columbia River islands west of Portland are attributed to the last Cascadia earthquake, circa A.D. 1700. Measured dikes from the cutbank sites east of Portland are tentatively correlated with the A.D. 1700 paleoliquefaction event in the western islands but are presently constrained to a broader interval: between A.D. 1500 and 1800.

For this reconnaissance survey we identify optimal fluidization sites in the Columbia River valley on the basis of thin mud caps over thick sand deposits, i.e., islands with cutbanks adjacent to main river channels. These optimal sites (R1, R4, R6, R7, R9, R12, R13, R14, R15, R17) confirm a regional decline of both dike abundance and maximum width over a west-east distance of about 120 km. Simple extrapolation from Figure 18 implies that small sills and rare dikes might have been produced in susceptible deposits further upstream beyond Pierce Island. Unfortunately, the river valley east of Pierce Island, i.e., the Columbia River gorge, is flooded by a series of impoundments.

Radiocarbon ages of wood fragments collected at or immediately above intruded dikes from sites R13 (250±70 RCYBP) and R17 (260±50 RCYBP) place the fluidization at these localities in latest prehistoric time. However, clear evidence of sand venting onto subaerial surfaces has not been established at any of the islands in the upper river valley. The apparent lack of such evidence might be attributed to poorer preservation potential, thicker mud caps, or less intense shaking relative to the islands of the lower river valley.

The "tephra" layers cut by dikes and sills in islands of the upper river valley are assumed to provide a maximum event age of 500 yr B.P., based on reported Mount St. Helens set W eruptions at about A.D. 1480 (Yamaguchi, 1985). Additional work is needed to verify the eruptive source of the apparent "tephra" layers in islands of the upper river valley. However, a radiocarbon date from charcoal in contact with a cut "tephra" layer exposed in the Sandy River delta (site R13) does yield an age (410±70 RCYBP) that is consistent with a Mount St. Helens set W eruptive source. If verified, these widespread "tephra" layers could provide important key beds for environmental and archaeological investigations in the islands of the Columbia River valley.

Sill-to-dike ratios

One of the general observations of this reconnaissance survey is the high proportion of clastic sills relative to clastic dikes in the central Cascadia margin. At several late Pleistocene sites (T4, T9, T10, T15, and T25), clastic sills are on the order of 10 times more abundant than clastic dike contacts in exposed outcrops. Clastic sills are interpreted to be more abundant than dikes in vibracores of the lower Columbia River islands (Peterson and others, 1994). The abundance of clastic sills increases to about 90 percent of the fluidization features exposed in cutbanks at localities of the upper Columbia River valley (sites R10–R17). The dominance of sills over dikes suggests that fluidization pore pressures were insufficient to penetrate capping layers and/or were laterally dissipated in permeable beds. We hypothesize that the large ratios of sills to dikes might reflect long duration of shaking at modest accelerations, which resulted in long duration of fluidization with moderately elevated pore pressures. Additional work is needed to evaluate the cyclic stress conditions that apparently favor clastic sill development at many localities in the central Cascadia margin.

Null-hypothesis test of M_W 8 subduction zone earthquakes

From the existing evidence of paleoliquefaction in the late Pleistocene marine terraces of Oregon and Washington, we find that the occurrence of subduction zone earthquakes in the M_W 8 range can not be ruled out for the central Cascadia margin. Specifically, the large size and abundance of fluidization features in the late Pleistocene marine terraces argue for strong coastal shaking in late Quaternary time. By comparison, the Cape Mendocino subduction-zone earthquake (M_W 7) is not reported to have produced cobble plumes, basal shears, or extensive lateral spreads (Prentice, Keefer, and Sims, 1992) as they were observed at some of the late Pleistocene paleoliquefaction sites. Such features could arise from shallow upper plate faults and/or from

deeper interplate earthquakes of larger magnitude. The results from this study do not discriminate between local and regional seismic sources for the paleoliquefaction localities in the late Pleistocene terrace deposits.

More diagnostic of potential earthquake magnitude in the central Cascadia margin is the inland extent of paleoliquefaction evidence in the Columbia River valley. Coseismic fluidization that is attributed to the A.D. 1700 Cascadia earthquake is traced up the lower river valley to Deer Island (Obermeier, 1995), a distance of about 85 km from the coast (Figure 10). Fluidization features that fall within a conservative time bracket of 150–500 yr B.P. are traced in the upper river valley to Pierce Island (site R17), a distance of about 150 km from the coast. Based on the 1992 Cape Mendocino earthquake (M_W 7), the possible 150-km extent of coseismic paleoliquefaction in the Columbia River exceeds that to be expected from a M_W 7 interplate rupture. However, this distance should be within reach of an interplate earthquake in the M_W 8 range, assuming local accelerations of 0.1 *g* (Anderson and others, 1994) and attenuation curves predicted for this margin (Geomatrix Consultants, Inc., 1995). Given these preliminary results, we cannot discount a M_W 8.5±0.5 earthquake for the last Cascadia dislocation event about 300 years ago.

A study of paleoliquefaction features produced by the 1964 great Alaskan earthquake (M_W 9) was recently performed, in part, for purposes of comparison to the Cascadia margin (Walsh and others, 1995). The study by Walsh and others concentrated on the preservation of dikes from reported liquefaction sites in fluvial-tidal settings. The forms and scales of fluidization features from the 1964 Alaskan earthquake are not substantially different from those of similar settings in the Cascadia marine terraces or the lower Columbia estuary. The larger fluidization features, i.e., wide dikes and lateral spreads, might be more abundant in the inland Alaska study areas (some 100 km from the coast) than at similar distances from the coast in this Cascadia reconnaissance survey.

Three points raised by Walsh and others (1995) are relevant to the geologic preservation potential of large dikes in fluvial-tidal settings. These points are that (1) large dikes mapped after the 1964 Alaskan earthquake were concentrated near channel margins, sites most susceptible to post-seismic channel erosion; (2) sand fillings in large dikes were selectively eroded by bottom currents following coseismic subsidence; and (3) dike occurrence was widely variable between liquefaction-susceptible areas of similar distance from the epicenter. These factors could diminish the apparent abundance of large clastic dikes in remnant marine terraces and eroded island outcrops of the Columbia River.

Regardless of earthquake magnitude or source, the scale and abundance of paleoliquefaction features along the Oregon coast and up the Columbia River are substantially greater than those produced by historic earthquakes in corresponding settings. For example, the coastal Cape Mendocino earthquake (1992) produced brief peak accelerations of 0.5 *g*, but liquefaction of susceptible deposits was limited to a 30-km radius of the main-shock epicenter. Paleoliquefaction produced by the Cascadia A.D. 1700 earthquake reached at least twice—and possibly five times—that distance inland from the coast. Historic earthquakes in the Portland basin area (Vancouver in 1962 and Scotts Mills in 1993) produced very brief peak accelerations of 0.1 *g*. Although they were locally damaging, these two earthquakes did not result in any reported evidence of liquefaction in susceptible deposits. By comparison, late prehistoric fluidization is widespread in susceptible deposits of the Columbia River islands for distances of at least 50 km both west and east of Portland. In summary, the use of historic earthquakes alone to establish regional or local seismic hazards in western Oregon understates the potential hazard of future earthquakes in the central Cascadia margin.

CONCLUSION

Evidence of strong shaking from cobble plumes, basal shears, lateral spreads, and clastic dikes and abundant sills is widely distributed in late Pleistocene marine terraces of the central Cascadia margin. The patchy distribution of large-scale fluidization features in the marine terraces appears to be related to the preservation and exposure of liquefaction-susceptible deposits. By comparison, no apparent correlations were found between the abundance of large clastic dikes, possible indicators of strong shaking, and relative position along the margin or proximity to mapped upper plate structures. Unfortunately, the late Pleistocene paleoliquefaction evidence from this reconnaissance survey does not discriminate between local or regional seismic sources along the coast.

Late Holocene paleoliquefaction sites in islands of the upper river valley of the Columbia River are tentatively correlated to the last Cascadia earthquake, circa A.D. 1700. This tentative correlation is based on (1) landward attenuation of dike abundance and width, (2) upper bounding radiocarbon dates, and (3) lower bounding "tephra" layers cut by the dikes. If the fluidization features in the upper river valley were produced by the A.D. 1700 Cascadia earthquake, then their distance from the coast (at least 150 km) would argue for a large subduction-zone earthquake (M_W 8.5±0.5).

Historic earthquakes (M_W 7.1 at Cape Mendocino and about M_W 5.5 near Portland) have not produced fluidization features that match the abundance, size, or extent of fluidization features from prehistoric events in corresponding settings of western Oregon. The recent historic earthquakes on the coast or in the Portland-Willamette Valley region do not provide adequate analogs for the local ground motions that could be expected from future earthquakes in the central Cascadia margin.

ACKNOWLEDGMENTS

Much of the paleoliquefaction mapping and vibracoring reported here was performed by undergraduate students in

the Geology Department at Portland State University. We particularly thank Doug Anderson, Scott Craig, Tara Karnes, Brian Peterson, John Siskowic, and Kristi Vockler for their assistance. Roger Hart, Tom Horning, Jim Phipps, Paul See, and other coastal geologists provided us with suggestions about paleoliquefaction sites on the coast. The Instrumental Neutron Activation Analysis (INAA) of tephra layers in the lower Columbia River was performed by Edward Gates. Marvin Beeson assisted with interpretation of the INAA data. This reconnaissance survey of paleoliquefaction evidence in the Cascadia margin was funded by the Oregon Department of Geology and Mineral Industries. Additional support for mapping cross sections in the late Pleistocene localities and for vibracoring in the lower Columbia River was provided under U.S. Geological Survey service contracts administered by Steve Obermeier and Brian Atwater, respectively. We thank Steve Obermeier for preliminary reviews of this manuscript.

REFERENCES CITED

Anderson, D.A., Soar, M., Peterson, C.D., and Mabey, M.A., 1994, Amplification modeling of possible coseismic liquefaction at the Sandy River delta, Troutdale, Oregon [abs.]: Oregon Academy of Science, Proceedings, v. 30, p. 39.

Atwater, B.F., 1987, Evidence for great Holocene earthquakes along the outer coast of Washington State: Science, v. 236, p. 942–944.

———1992, Geologic evidence for earthquakes during the past 2,000 years along the Copalis River, southern coastal Washington: Journal of Geophysical Research, v. 97, p. 1901–1919.

———1994, Geology of Holocene liquefaction features along the lower Columbia River at Marsh, Brush, Price, Hunting, and Wallace Islands, Oregon and Washington: U.S. Geological Survey Open-File Report 94–209, 64 p.

Barnes, M.L., 1995, Geochemistry of the Boring Lava along the west side of the Tualatin Mountains and of sediments from drill holes in the Portland and Tualatin basins, Portland, Oregon: Portland, Oreg., Portland State University master's thesis, 182 p.

Black, G.L., 1996, Earthquake intensity maps for the March 25, 1993, Scotts Mills, Oregon, earthquake: Oregon Geology, v. 58, no. 2, p. 35–41.

Bott, J.D.J., and Wong, I.G., 1993, Historical earthquakes in and around Portland, Oregon: Oregon Geology, v. 55, no. 5, p. 116–122.

Briggs, G.G., 1994, Coastal crossing of the elastic strain zero-isobase, Cascadia margin, south-central Oregon coast: Portland, Oreg., Portland State University master's thesis, 251 p.

Clifton, H.E., 1994, Transgressive and early highstand systems tracts: Pleistocene terrace deposits, Willapa Bay, Washington: Field Trip Guide SEPM Research Conference, Clastic Deposits of the Transgressive Systems Tract, Long Beach, Wash., 1994.

Craig, W.S., Peterson, C.D., Travis, P., Meek, M., Wieneke, D., Soar, M., and Bertelling, J., 1993, Shallow subsurface stratigraphy of late Holocene coseismic liquefaction sites in the Columbia River, Central Cascadia margin, USA [abs.]: EOS, v. 74, no. 43 suppl., p. 199.

Darienzo, M.E., 1991, Late Holocene paleoseismicity along the northern Oregon coast: Portland, Oreg., Portland State University doctoral dissertation, 167 p.

Darienzo, M.E., and Peterson, C.D., 1995, Magnitude and frequency of subduction-zone earthquakes along the northern Oregon coast in the past 3,000 years: Oregon Geology, v. 57, no. 1, p. 3–12.

Fiegel, G.L., and Kutter, B.L., 1994, Liquefaction mechanism for layered soils: Journal of Geotechnical Engineering, ASCE, v. 120, p. 737–755.

Florer, L.E., 1972, Quaternary paleoecology and stratigraphy of the sea cliffs, western Olympic Peninsula, Washington: Quaternary Research, v. 2, p. 202–216.

Gates, E.B., 1994, The Holocene sedimentary framework of the lower Columbia River basin: Portland, Oreg., Portland State University master's thesis, 210 p.

Geomatrix Consultants, Inc., 1995, Seismic design mapping, State of Oregon: Final report to Oregon Department of Transportation, Project no. 2442, var. pag.

Goldfinger, C., Kulm, L.D., Yeats, R.S., Mitchell, C., Weldon, R., II, Peterson, C., Darienzo, M., Grant, W., and Priest, G.R., 1992, Neotectonic map of the Oregon continental margin and adjacent abyssal plain: Oregon Department of Geology and Mineral Industries Open-File Report O-92-4, 17 p., 2 plates.

Holzer, T.L., and Clark, M.M., 1993, Sand boils without earthquakes: Geology, v. 21, p.873–876.

Jaeger, H.M., Nagel, S.R., and Behringer, R.P., 1996, The physics of granular materials: Physics Today, v. 49, no. 4, p. 32–38.

Jayko, A.S, Marshall, G.A., and Carver, G.A., 1992, Elevation changes [Cape Mendocino earthquakes of April 25–26, 1992]: Earthquakes and Volcanoes, v. 23, no. 3, p. 139–143.

Kelsey, H.M., 1990, Late Quaternary deformation of marine terraces on the Cascadia subduction zone near Cape Blanco, Oregon: Tectonics, v. 9, p. 983–1014.

Kelsey, H.M., Witter, R.C., and Polenz, M., 1993, Cascadia paleoseismic record derived from late Holocene fluvial and lake sediments, Sixes River Valley, Cape Blanco, south coastal Oregon [abs.]: EOS, v. 74, no. 43 suppl., p. 199.

Kennedy, G.L., Lajoie, K.R., and Wehmiller, J.F., 1982, Aminostratigraphy and faunal correlations of late Quaternary marine terraces, Pacific coast, USA: Nature, v. 299, p. 545–547.

Kolb, C.R., 1976, Geologic control of sand boils along Mississippi River levees, *in* Coats, D.R., ed., Geomorphology and engineering: Halstead Press, p. 99–114.

Madin, I.P., McInelly, G.W., and Kelsey, H.M., 1995, Geologic map of the Charleston quadrangle, Coos County, Oregon: Oregon Department of Geology and Mineral Industries Geological Map Series GMS–94, scale 1:24,000.

Madin, I.P., Priest, G.R., Mabey, M.A., Malone, S., Yelin, T.S., and Meier, D., 1993, March 25, 1993, Scotts Mills earthquake—western Oregon's wake-up call: Oregon Geology, v. 55, no. 3, p. 51–57.

McInelly, G.W., and Kelsey, H.M., 1990, Late Quaternary tectonic deformation in the Cape Arago-Bandon region of coastal Oregon as deduced from wave-cut platforms: Journal of Geophysical Research, v. 95, no. B5, p. 6699–6713.

Michael, A., Oppenheimer, D., and Reasenberg, P., 1992, Preliminary seismological results [Cape Mendocino earthquakes of April 25–26, 1992]: Earthquakes and Volcanoes, v. 23, no. 3, p. 110–115.

Mulder, R.A., 1992, Regional tectonic deformation of the northern Oregon coast as recorded by Pleistocene marine terraces: Portland, Oreg., Portland State University master's thesis, 96 p.

Muhs, D.R., Kelsey, H.M., Miller, G.H., Kennedy, G.L., Whelan, J.F., and McInelly, G.W., 1990, Age estimates and uplift rates for late Pleistocene marine terraces: Southern Oregon portion of the Cascadia forearc: Journal of Geophysical Research, v. 95, no. B5, p. 6685–6698.

Mullineaux, D.R., 1986, Summary of pre-1980 tephra-fall deposits erupted from Mount St. Helens, Washington State, USA: Bulletin of Volcanology, v. 48, no. 1, p. 17–26.

Nabelek, J., and Xia, G., 1995, Moment-tensor analysis using regional data: Application to the 25 March, 1993, Scotts Mills, Oregon earthquake: Geophysical Research Letters, v. 22, p. 13–16.

Nataraja, M.S., and Gill, H.S., 1983, Ocean-wave-induced liquefaction analysis: Journal of Geotechnical Engineering, ASCE, v. 109, p. 573–590.

National Research Council, 1985, Liquefaction of soils during earthquakes: Washington D.C., National Academy Press, 240 p.

Obermeier, S.F., 1995, Preliminary estimates of the strength of prehistoric shaking in the Columbia River valley and the southern half of coastal Washington, with emphasis for a Cascadia subduction zone earthquake about 300 years ago: U.S. Geological Survey Open-File Report 94–589, 46 p.

———1996, Use of liquefaction-induced features for paleoseismic analysis. An overview of how seismic liquefaction features can be distinguished from other features and how regional distribution and properties of source sediment can be used to infer the location and strength of Holocene paleoearthquakes: Engineering Geology, v. 44, p. 1–76.

Obermeier, S.F., Atwater, B.F., Benson, B.E, Peterson, C.D., Moses, L.J., Pringle, P.T., and Palmer, S.P., 1993, Liquefaction about 300 years ago along tidal reaches of the Columbia River, Oregon and Washington [abs.]: EOS, v. 74, no. 43 suppl., p. 198.

Oppenheimer, D., Beroza, G., Carver, G., Dengler, L., Eaton, J., Gee, L., Gonzalez, F., Jayko, A., Li, W.H., Lisowski, M., Magee, M., Marshall, G., Murray, M., McPherson, R., Romanowicz, B., Satake, K., Simpson, R., Somerville, P., Stein, R., and Valentine, D., 1993, The Cape Mendocino, California, earthquakes of April 1992: Subduction at the Triple Junction: Science, v. 261, p. 433–438.

Palmer, S.P., 1990, Geotechnical analysis of liquefaction in Puyallup during the 1949 and 1965 Puget Sound earthquakes: Washington Geologic Newsletter, v. 18, no. 3, p. 3–7.
Peterson, B., Peterson, C.D., Vockler, K., Wyatt, J., Marsh, M., Rose, G., and Horning, T., 1994, Vibracore subsurface investigation of a late Holocene liquefaction site in the central Cascadia margin: Hunting Island, Columbia River, Washington: Unpublished field study report to U.S. Geological Survey, 12 p.
Peterson, C.D., Darienzo, M.E., Pettit, D.J., Jackson, P., and Rosenfeld, C., 1991, Littoral cell development in the convergent Cascadia margin of the Pacific Northwest, USA, *in* Osborne, R.H., ed., From shoreline to abyss: Contributions to marine geology in honor of Francis Parker Shepard: Society for Sedimentary Geology (SEPM) Special Publication 46, p. 17–34.
Peterson, C.D., Hansen, M., and Jones, D., 1991, Widespread evidence of paleoliquefaction in late Pleistocene marine terraces from the Oregon and Washington margins of the Cascadia subduction zone [abs.]: EOS, v. 72, no. 44 suppl, p. 313.
Peterson, C.D., and Madin, I.P., 1992. Variation in form and scale of paleoliquefaction structures in late Pleistocene deposits of the central Cascadia margin [abs.]: Geological Society of America Abstracts with Programs, v. 24, no. 5, p. 74.
Peterson, G.L., 1968. Flow structures in sandstone dikes: Sedimentary Geology, v. 2, p. 177–190.
Pirazzoli, P.A., 1993, Global sea-level changes and their measurement: Global and Planetary Change, v. 8, p. 135–148.
Prentice, C.S., Keefer, D.K, and Sims, J.D., 1992, Surface effects of the earthquakes [Cape Mendocino earhquakes of April 25–26, 1992]: Earthquakes and Volcanoes, v. 23, no. 3, p. 127–134.
Rau, W.W., 1973, Geology of the Washington coast between Point Grenville and the Hoh River: Washington Division of Geology and Earth Resources Bulletin 66, 58 p.
Saucier, R.T., 1989, Evidence for episodic sand-blow activity during the 1811–1812 New Madrid (Missouri) earthquake series: Geology, v. 17, no. 2, p. 103–106.
Seed, H.B., and Idriss, I.M., 1982, Ground motions and soil liquefaction during earthquakes: Earthquake Engineering Research Institute Monograph, 134 p.
Seed, H.B., Tokimatsu, K., Harder, L.F., and Chung, R.M., 1985, Influence of SPT procedures in soil liquefaction resistance evaluations: Journal of Geotechnical Engineering, ASCE, v. 111, p. 1425–1445.
Shulene, J.A., 1990, Evidence of liquefaction in the Puyallup Valley: Washington Geologic Newsletter, v. 18, no. 2, p. 15–16.
Stokoe, K.H., Andrus, R.D., Rix, G.J., Sanchez-Salinero, I., Sheu, J.C., and Mok, Y.J., 1988, Field investigation of gravelly soils which did and did not liquefy during the 1983 Borah Peak, Idaho, earthquake: Austin, Tex., University of Texas Geotechnical Engineering Center, Geotechnical Engineering Report GR87–1, 206 p.
Siskowic, J.D., Anderson, D.A., Peterson, B., Peterson, C.D., Soar, M., Travis, P., and Vockler, K., 1994, Possible coseismic liquefaction evidence at the Sandy River delta, Portland, Oregon: Tentative correlation with the last great Cascadia rupture [abs.]: Geological Society of America Abstracts with Programs, v. 26, no. 2, p. 92.
Ticknor, R., 1993, Late Quaternary crustal deformation on the central Oregon coast as deduced from uplifted wave-cut platforms: Bellingham, Wash., Western Washington University master's thesis, 70 p.
Tuttle, M., and Seeber, L., 1991, Historic and prehistoric earthquake-induced liquefaction in Newbury, Massachusetts: Geology, v. 19, p. 594–597.
Vockler, K., Anderson, D., Peterson, B., Peterson, C., Siskowic, J., Soar, M., and Travis, P., 1994, Discrimination of liquefaction-inducing events (lahar, flood, and seismic) at the Sandy River delta, Troutdale, Oregon [abs.]: Geological Society of America Abstracts with Programs, v. 26, no. 2, p. 101.
Walsh, T.J., Combellick, R.A., and Black, G.L., 1995, Liquefaction features from a subduction zone earthquake: Preserved examples from the 1964 Alaska earthquake: Washington Division of Geology and Earth Resources Report of Investigations 32, 80 p.
Yamaguchi, D.K., 1985, Tree-ring evidence for a two-year interval between recent prehistoric explosive eruptions of Mount St. Helens: Geology, v. 13, no. 8, p. 554–557.
Yelin, T.S., and Patton, H.J., 1991, Seismotectonics of the Portland, Oregon, region: Seismological Society of America Bulletin, v. 81, no. 1, p. 109–130.
Youd, T.L., 1991. Mapping of earthquake-induced liquefaction for seismic zonation, *in* International Conference on Seismic Zonation, 4th, August 1991, Stanford, Calif., Proceedings: Oakland, Calif., Earthquake Engineering Research Institute, p. 111–147. □

DOGAMI PUBLICATIONS AND RELEASES

Released April 24, 1997

Estimates of Coastal Subsidence from Great Earthquakes in the Cascadia Subduction Zone, Vancouver Island, B.C., Washington, Oregon, and Northernmost California, by a team of scientists from Portland State University, Humboldt State University, and the Geological Survey of Canada. Open-File Report O-97-05, 19 p. text and illustrations, 25 p. tabular data, $6.

The report presents estimates of drops in ground level (subsidence) that can be caused by great earthquakes along the Pacific Northwest coast. The results can aid in the evaluation of shoreline erosion and coastal flooding that might result from earthquake-related subsidence.

Great subduction-zone earthquakes can result in coastal subsidence of up to a few meters and cause coastal flooding and beach erosion that may persist for decades. It has been estimated that an earthquake-related subsidence of 75 cm (about 30 inches) at Siletz Bay would cause 50 m (about 55 yards) of beach retreat. Such catastrophic beach erosion would lead to faster undercutting of bluffs and failures of sea cliffs.

Estimates of subsidence were derived from the study of various indicators of past changes in tide levels, such as buried peat and certain fossils. Data in the report were obtained from more than a dozen different studies supported by U.S., State, and Canadian Provincial grants and contracts during the last ten years. The final compilation was supported by the National Oceanic and Atmospheric Administration (NOAA) and by appropriations made by the Oregon State Legislature.

The following release is available for inspection in the libraries of the DOGAMI offices in Portland and Grants Pass. It is not published in multiple copies and is not for sale but limited to library access only. Photocopies may be obtained at cost.

Released April 21, 1997

Preliminary Geologic Map of the Southwest Part of the Medford 30 × 60 Minute Quadrangle, Oregon and California, by Jad D'Allura, Southern Oregon State College, in cooperation with DOGAMI. Open-File Report O–97–03, 1 map sheet (scale 1:100,000), 23 p. text. Library access only.

The area covered extends approximately from Ashland toward the southwest to the Siskiyou Mountains and the California border and includes eight 7½-minute quadrangles: Sterling Creek, Talent, Ashland, Emigrant Lake, Siskiyou Pass, Mount Ashland, Siskiyou Peak, and Dutchman Peak. The text contains explanations of the rock units presented on the map, the geologic history, composition, and structure, and radiometric age determinations of 15 samples collected in the area. □

About predicting earthquakes

Earthquakes cannot be predicted. This is the considered conviction of scientists Robert J. Geller of Tokyo University, David D. Jackson and Yan Y. Kagan of the University of California at Los Angeles, and F. Mulargia of the University of Bologna. In the March 14, 1997, issue of *Science* they discuss the consensus of a meeting on the subject that was held in London in late 1996.

- Faults, the places where earthquakes originate, are "notoriously intractable," i.e., they are generally inaccessible to direct measurements.
- It would be, of course, most valuable to be able to predict large earthquakes. However, the current assessment is that the Earth is "in a state of self-organized criticality," which means that any small earthquake could develop into a large one. The uncountable details that make up the initial conditions for a given earthquake in a given place and time may come from an area much broader than just the immediate vicinity of the fault. Being able to know all the relevant details is so highly unlikely as to be inherently impossible—aside from the fact that we have no theory that can analyze such data and arrive at a prediction.
- The various "anomalous" phenomena that have been offered as precursors to earthquakes cannot reasonably be claimed as such. Their significance was "seen" only after the event; they do not show consistent patterns; and there are no definitions, physical mechanisms, or statistics that would allow a correlation between the alleged precursors and earthquakes.
- Claims that, in China, one earthquake in 1975 was successfully predicted are questionable, because the claim that "very few people were killed" conflicts with official reports of over 1,300 deaths and almost 17,000 injuries. Reports on that earthquake may have been distorted under political pressure. A swarm of microearthquakes beginning over 24 hours before the main shock may have done enough to motivate people to evacuate spontaneously.
- A scientific theory linking geoelectric observations with earthquakes in Greece has been found to be without scientific merit.
- The question that remains is whether prediction of earthquakes is "inherently impossible or just fiendishly difficult." But in practice, the difference does not matter. In view of the unsuccessful attempts over more than 100 years, continued thorough scientific research would require so much effort that it "seems unwise to invest heavily in monitoring possible precursors."

However, while prediction does not seem to be a worthwhile goal to pursue, hazard mitigation does profit from scientific efforts. Statistical estimates of expected seismicity and expected strong ground motion can be developed as data for earthquake preparedness, such as the designing of earthquake-resistant structures. The ability to quickly determine sources and magnitudes of earthquakes will help with disaster relief efforts. Being able to warn coastal areas of tsunamis from undersea earthquakes will save many lives. Such efforts are indeed "where earthquake research can greatly benefit the public." □

Geologic-hazard slide sets available

The National Geophysical Data Center of the National Oceanic and Atmospheric Administration (NOAA) offers a variety of educational slide sets depicting the effects of earthquakes, tsunamis, landslides, and volcanic eruptions. Each of the sets costs $30 and consists of 20 slides in color or black-and-white, documentation that provides background material, dates, locations, and descriptions of effects for the depicted hazards. The slides are suitable for both technical and nontechnical audiences. We are reprinting a partial list of what is available.

Landslides

Depicts diverse types of landslides and mass wasting. Photos were taken at various locations in the United States, Canada, Australia, Peru, and Switzerland. Of particular interest are views of the famous 1903 rock slide at Frank, Alberta, Canada, that covered the town of Frank in less than two minutes, and the 1970 earthquake-induced rock and snow slide that buried the towns of Yungay and Ranrahirca in Peru. (Color; 647-A11-006)

Earthquake damage—general

Illustrates several kinds of effects caused by 11 earthquakes in seven countries and four states in the United States. Pictures show surface faulting, landslides, soil liquefaction, and structural damage. This set is designed to give an overview and summary of earthquake effects. (Color; 647-A11-001)

Earthquake damage, San Francisco, California, April 18, 1906

Includes a panoramic view of San Francisco in flames a few hours after the earthquake, damage scenes from the area, and other unique photographs. (B&W; 647-A11-002)

Earthquake damage, Mexico City, September 1985

Shows different types of damaged buildings and major kinds of structural failure including collapse of top, middle, and bottom floors and total building failure. The effect of the subsoils on the earth's shaking and on building damage is emphasized. (Color; 647-A11-003)

Earthquake damage, Loma Prieta, October 1989, Set 1—Loma Prieta vicinity

Includes damage in Boulder Creek, Aptos, Los Gatos, San Jose, Santa Cruz, Scott's Valley, and Watsonville. The slides also depict earth cracks and structural damage to

homes in the Santa Cruz mountains. (Color; 641-A11-012)

Set 2—San Francisco and Oakland

Highlights the damage in the Marina area of San Francisco. The set also includes photographs of the damaged building in the area south of Market Street where five deaths occurred, the now famous damage to the San Francisco-Oakland Bay Bridge, and the Cypress Section of the Nimitz Freeway (I-880) where 41 deaths occurred. (Color; 647-A11-013)

Earthquake damage, Northridge, January 17, 1994

Set 1—Community of Northridge

This set of slides depicts the damage in the immediate area of the epicenter of this destructive earthquake. Photos showing damage to shopping centers, parking garages, and the interior and exterior of apartment buildings are included. (Color; 647-A11-018)

Set 2—Communities other than Northridge

This set of slides depicts some of the severely damaged structures in Sylmar, Fillmore, Granada Hills, Reseda, Van Nuys, Sherman Oaks, Chatsworth, Santa Monica, and Los Angeles. (Color; 641- A11-019)

Earthquake damage to transportation systems

Depicts earthquake damage to streets, highways, bridges, overpasses, and railroads caused by 12 earthquakes in Guatemala, Japan, Mexico, Armenia, and five states in the United States. Views of structural damage to the San Francisco-Oakland Bay bridge and the Nimitz Freeway (I-880) sustained in the October 1989 earthquake are included. (B&W/color; 641- A11-004)

Earthquake damage to schools

Nine destructive earthquakes that occurred in the United States and eight earthquakes that occurred in foreign countries from 1886 to 1988 are depicted. The set graphically illustrates the potential danger that major earthquakes pose to school structures. The photograph taken in 1886 of the damage at Charleston College, Charleston, South Carolina, is of special interest since it is an illustration of earthquake damage possible on the east coast of the United States. (B&W/color; 647-A11- 005)

Earthquake damage, great Alaska earthquake, March 1964

Shows geologic changes; damage to structures, transportation systems, and utilities; and tsunami damage. Features the effects of four major landslides in Anchorage, including the Fourth Avenue and Turnagain Heights landslides. (Color; 641-A11-007)

Earthquake damage, southern California, 1979–1989

Shows earthquake damage from the following events: Imperial Valley, 1979; Westmorland, 1981; Palm Springs, 1986; and Whittier, 1987. Partially and totally collapsed buildings resulting from the Whittier Narrows earthquake are shown. (Color; 647-A11-008)

Earthquake damage, central California, 1980-1984

Shows earthquake damage from the following events: Livermore, 1980; Coalinga, 1983; and Morgan Hill, 1984. Several totally and partially collapsed buildings in the downtown area of Coalinga are shown. (Color; 641-A11-009)

Earthquake damage, Armenian SSR, December 1988

Includes damage photographs taken in and around the devastated cities of Spitak and Leninakan, where 25,000 deaths occurred. Illustrates the structural types that were vulnerable to failure. This set shows that inadequate building construction combined with shaking from a moderate earthquake can result in high death tolls and tremendous economic loss. (Color; 647- A11-011)

Earthquake damage, northern Iran, June 21, 1990, engineering aspects

This set depicts damage resulting from intensive ground motion and soil liquefaction. It shows damage to buildings of various types, including unreinforced masonry, steel structures, and concrete buildings. Damage to infrastructure is also shown. (Color; 647-A11-014)

Earthquake damage, the Cape Mendocino earthquakes, April 25 and 26, 1992

Illustrates effects of a moderately large earthquake and moderate aftershocks in a sparsely settled area. Includes damage in Rio Dell, Scotia, Honeydew, Petrolia, and Ferndale, California. (Color; 647-A11-016)

Earthquake damage, the Landers and Big Bear earthquakes, June 28, 1992

Damage photos from a magnitude 7.6 earthquake in southern California and a magnitude 6.7 earthquake occurring 17 miles away about three hours later. Examples of structural damage, liquefaction, surface faulting, and landslides. (Color; 641-A11-011)

Earthquake damage, the San Fernando Valley earthquakes, February 9, 1971, and January 17, 1994

This set of slides compares and contrasts these two earthquakes that were separated by ten miles and about 23 years. Disproving the notion that once an earthquake has occurred, an area is "safe" from future earthquakes, these two events affected much of the same area and even some of the same structures. (Color; 647-A11-020)

Tsunamis—general

Depicts advancing waves, harbor damage, and structural damage from seven tsunami events that have occurred since 1946 in the Pacific region. The set includes before-and-after views of Scotch Cap Lighthouse (the Aleutian Islands), which was completely washed away by a wave of

more than 30 meters. A somewhat out-of-focus, but nevertheless unique photograph of a man about to be inundated by a huge wave that destroyed the Hilo, Hawaii, waterfront is also included. (B&W/Color; 648-A11-001)

The major tsunamis of 1992—Nicaragua and Indonesia

The slide set shows damage from the two major tsunami events of 1992—the September tsunami along Nicaragua's Pacific coast (6 slides), and the December tsunami in the Flores region of Indonesia (14 slides). The slides illustrate how a tsunami may affect an area economically and ecologically. (Color; 64S-A11-002)

The Hokkaido Nansei-Oki tsunami, July 12, 1993

The slides show the result of one of the largest tsunamis in Japan's history. It caused spectacular localized damage, especially on the southwestern shores of Hokkaido, and on Okushiri Island. The set includes views of damage to ships, dwellings, and businesses and unique views of clocks stopped in time by the tsunami. (Color; 648-A11-003)

Most of the slide sets, except for the more recent ones, have been digitally scanned and replicated on a two-volume CD-ROM set (1115-A27-001) that sells for $71.

Images on the CDs are in both a 24-bit TIF image and a compressed 8-bit PCX image. Included with each image is the caption. These images can be imported into many standard software packages. Windows-based access software, for PCX images only, is provided. Please note that the display quality of these images is strongly influenced by the resolution of your computer's graphic card.

These slide sets and similar ones on volcanic hazards can be ordered from

National Geophysical Data Center
NOAA, E/GC1, Dept 953
325 Broadway
Boulder, CO 80303, U.S.A.
Phone: 303-497-6607
Fax: 303-497-6513
Voice/TDD: 303-497-6958
Telex: 592811 NOAA MASC BDR
Internet: info@ngdc.noaa.gov

U.S. Department of Commerce regulations require prepayment on all orders, with the exception of orders from U.S. agencies. Also, due to recent legislation, prices are subject to change without notice. Call for price verification. Please refer to the product number when ordering.

Make checks and money orders payable to COMMERCE/NOAA/NGDC. Do not send cash. All non-U.S.A. orders must be in U.S. Dollars drawn on a U.S.A. bank. A ten-dollar ($10) handling fee is required for delivery outside the U.S.A. Orders may be charged to American Express, MasterCard, or VISA by phone, letter, or fax. Please include a credit card account number, expiration date, telephone number, and your signature with your order. □

THESIS ABSTRACTS

The Oregon Department of Geology and Mineral Industries maintains a collection of theses and dissertations on Oregon geology. From time to time, we print abstracts of new acquisitions that in our opinion are of general interest to our readers.

Vertical component of present-day deformation in the western Pacific Northwest, by Clifton Edwards Mitchell (M.S., University of Qregon, 1992), 103 p.

This thesis maps the regional pattern of vertical deformation of the Pacific Northwest west of the Cascade Range and, using long-term tidal records from Crescent City, Astoria, and Neah Bay, assigns uplift rates to that pattern to reference it to the geoid. Relative uplift profiles along the coast are constructed from two independent data sets that indicate crustal motion: comparison of records from eight tide gauges, and comparison of releveling surveys. Both methods detect only relative motion, but the two entirely independent data sets produce comparable profiles along the coast. The releveling data set allows construction of profiles inland from the coast, and these various profiles are assembled into a network of relative uplift rates. A contoured map of this relative network is combined with uplift rates at three long-term tidal stations to contour a map of regional uplift rates relative to the geoid.

Numerical modeling of tsunamis with applications to the Sea of Japan and the Pacific Northwest, by Edward P. Myers, III (M.S., Oregon Graduate Institute of Science and Technology, 1994), 161 p.

Recent evidence along the Oregon and Washington coastlines suggests that the Pacific Northwest experiences great subduction earthquakes every 200 to 600 years. Such events appear to occur as the Juan de Fuca tectonic plate subducts beneath the North American plate in what is termed the Cascadia Subduction Zone. These earthquakes are estimated to range between 8 and 9 on the magnitude scale and cause sufficient displacement in the sea floor to generate large tsunamis.

This evidence provides the incentive for numerical modeling of tsunamis. Two test cases are used as the framework for evaluating the ability of a numerical model to represent tsunami wave activity. A finite element approach is used that shows that a wave continuity formulation is capable of handling such tsunami simulations. Details of initial and boundary conditions are provided, taking into account a moving sea floor and allowing waves to travel undisturbed though transmissive boundaries.

Principles of mass conservation and energy conservation are used as benchmarks for how well the physics is represented in the systems. Such results have historically not been presented in numerical studies of tsunamis. A detailed evaluation of them here shows that mass is generally well conserved while energy is not. Some of the energy loss can

be taken into account by energy leaving the domain through transmissive boundaries, yet problems still occur during the early time steps, when initial conditions have been imposed and when the waves interact with land boundaries. My interpretation is that both of these situations are ones in which vertical accelerations are important. However, the shallow-water equations assume a hydrostatic approximation that neglects pressure gradients due to vertical accelerations. It is therefore possible that the shallow-water equations do not inherently conserve energy.

The July 7, 1993, Hokkaido Nansei-Oki tsunami is used to test the ability of the model to reproduce observed wave forms at tidal gauge stations. This involves calibration with respect to seismic source scenarios, friction, and diffusion. Wave forms are reasonably reproduced at near-field stations, yet far-field stations show differences in amplitude and wavelength. If the width and length of the fault plane are correctly specified, the numerical results at near-field stations suggest that fault plane models are able to generate initial conditions quite well.

Two seismic source scenarios are then considered for the Pacific Northwest. Wave forms are computed for various coastal locations, and patterns of energy distribution are displayed. Such information should be useful for coastal communities in terms of what types of waves would be arriving near their portion of the coastline and what regions may be more susceptible to energy focusing. Uncertainty remains, in particular regarding the source mechanism, because computed subsidence from fault plane models for both scenarios is less than what field evidence from past subduction events suggests. □

History of mapping can be a puzzle

Some time not too long ago, we tried to determine the location of a 1960 master's thesis in the DOGAMI library collection. The title said, "northwest quarter Alvord Lake Three quadrangle," but we could not find any record of a quadrangle by that name. Finally, Peter Stark of the University of Oregon map library responded to our call for help with the following explanation:

"We have a 1946 U.S. Army Corps of Engineers topo map index/progress sheet for Oregon/Washington/Idaho/western Montana. In places where no mapping was completed or even started or projected, the Corps went ahead and named all the possible 30-minute quadrangles. The Alvord Lake 30-minute quadrangle was named at that time.

"In keeping with the military way of numbering quadrangles even further to describe larger scale mapping, the numbers 1, 2, 3, or 4 were added to the 30-minute name to designate 15-minute maps (Alvord Lake 1 = NE 15-minute segment, 2 = NW, 3 = SW, 4 = SE). Even though Alvord Lake and many other quadrangle maps numbered in this way were never published, the name/number system served as a locating convention for many years.

"Our student used this convention to describe the area he mapped, even though there was no topographic mapping for this area. [He used a base map by the Oregon State Highway Department—ed.]

"Applying this scheme to the northwest quarter of the Alvord Lake Three quadrangle, I come up with the modern USGS quadrangle name 'Robbers Roost' . . ."

Indeed, this area was not mapped until production of the familiar USGS topographic maps had progressed to 7½-minute coverage. Only at the 7½-minute level do we have complete topographic coverage of the state of Oregon. The historic event of finishing this work came 1991, after a 42-year effort (see *Oregon Geology* of May 1990). □

BOOK REVIEW

by Beverly F. Vogt

Fire, Faults and Floods: A Road and Trail Guide Exploring the Origins of the Columbia River Basin, by Marge and Ted Mueller, 1997, University of Idaho Press, paperback, 288 p., $19.95

This wonderful little book tells two geologic stories—the story of the Columbia River Basalt Group and the story of the catastrophic floods from Glacial Lake Missoula. It covers the Columbia River country from Montana to the Pacific Ocean. The introductory section introduces the reader to plate tectonics, the Glacial Lake Missoula Floods, some general concepts of the regional geology, and the Columbia River Basalt Group. Each of the ten chapters that follow introduces the geology of a specific area, along with descriptions of interesting roads or trails to follow. Included are 95 photos and 80 maps and illustrations.

If you were ever curious about the geology of the area covered by the book, this is the way to find out about it. If you already have a nodding acquaintance with the geology but have ever wondered such things as the story of the Blue Lake Rhino, which Columbia River basalt flows reached the coast, how Grand Coulee was formed, where the ancestral Columbia River flowed, or where to find ring dikes or giant ripple marks from the Missoula floods, this is the book for you. It has maps and directions on how to reach these and many other interesting features—and as a bonus provides diagrams explaining how they formed.

The authors have written ten other books on the Pacific Northwest. The geology in this book is presented in nontechnical terms and is accompanied with other information about such topics as history, plant life, wild life, petroglyphs, and recreational opportunities. One of the authors confesses that before he was bitten by the geology bug, he thought the scenery of area was "unendingly boring." Luckily for us, he and his wife learned about geology and chose to share what they learned—because if you travel through the Columbia River Basin with this book in hand, you will be introduced to a variety of wonders that you never suspected existed. *Fire, Faults and Floods* may be purchased from the Nature of the Northwest Information Center or your neighborhood book seller. □

AVAILABLE PUBLICATIONS
OREGON DEPARTMENT OF GEOLOGY AND MINERAL INDUSTRIES

GEOLOGICAL MAP SERIES

GMS-5 Powers 15' quadrangle, Coos and Curry Counties. 1971 — 4.00
GMS-6 Part of Snake River canyon. 1974 — 8.00
GMS-8 Complete Bouguer gravity anomaly map, central Cascades. 1978 — 4.00
GMS-9 Total-field aeromagnetic anomaly map, central Cascades. 1978 — 4.00
GMS-10 Low- to intermediate-temperature thermal springs and wells. 1978 — 4.00
GMS-12 Oregon part, Mineral 15' quadrangle, Baker County. 1978 — 4.00
GMS-13 Huntington/Olds Ferry 15' quads., Baker/Malheur Counties. 1979 — 4.00
GMS-14 Index to published geologic mapping in Oregon, 1898-1979. 1981 — 8.00
GMS-15 Gravity anomaly maps, north Cascades. 1981 — 4.00
GMS-16 Gravity anomaly maps, south Cascades. 1981 — 4.00
GMS-17 Total-field aeromagnetic anomaly map, south Cascades. 1981 — 4.00
GMS-18 Rickreall, Salem West, Monmouth, and Sidney 7½' quadrangles, Marion and Polk Counties. 1981 — 6.00
GMS-19 Bourne 7½' quadrangle, Baker County. 1982 — 6.00
GMS-20 S½ Burns 15' quadrangle, Harney County. 1982 — 6.00
GMS-21 Vale East 7½' quadrangle, Malheur County. 1982 — 6.00
GMS-22 Mount Ireland 7½' quadrangle, Baker/Grant Counties. 1982 — 6.00
GMS-23 Sheridan 7½' quadrangle, Polk and Yamhill Counties. 1982 — 6.00
GMS-24 Grand Ronde 7½' quadrangle, Polk/Yamhill Counties. 1982 — 6.00
GMS-25 Granite 7½' quadrangle, Grant County. 1982 — 6.00
GMS-26 Residual gravity, north/central/south Cascades. 1982 — 6.00
GMS-27 Geologic and neotectonic evaluation of north-central Oregon. The Dalles 1° × 2° quadrangle. 1982 — 7.00
GMS-28 Greenhorn 7½' quadrangle, Baker/Grant Counties. 1983 — 6.00
GMS-29 NE¼ Bates 15' quadrangle, Baker/Grant Counties. 1983 — 6.00
GMS-30 SE¼ Pearsoll Peak 15' quad., Curry/Josephine Counties. 1984 — 7.00
GMS-31 NW¼ Bates 15' quadrangle, Grant County. 1984 — 6.00
GMS-32 Wilhoit 7½' quadrangle, Clackamas/Marion Counties. 1984 — 5.00
GMS-33 Scotts Mills 7½' quad., Clackamas/Marion Counties. 1984 — 5.00
GMS-34 Stayton NE 7½' quadrangle, Marion County. 1984 — 5.00
GMS-35 SW¼ Bates 15' quadrangle, Grant County. 1984 — 6.00
GMS-36 Mineral resources of Oregon. 1984 — 9.00
GMS-37 Mineral resources, offshore Oregon. 1985 — 7.00
GMS-38 NW¼ Cave Junction 15' quadrangle, Josephine County. 1986 — 7.00
GMS-39 Bibliography and index: ocean floor, continental margin. 1986 — 6.00
GMS-40 Total-field aeromagnetic anomaly maps, northern Cascades. 1985 — 5.00
GMS-41 Elkhorn Peak 7½' quadrangle, Baker County. 1987 — 7.00
GMS-42 Ocean floor off Oregon and adjacent continental margin. 1986 — 9.00
GMS-43 Eagle Butte & Gateway 7½' quads., Jefferson/Wasco C. 1987 — 5.00
as set with GMS-44 and GMS-45 — 11.00
GMS-44 Seekseequa Junct./Metolius B. 7½' quads., Jefferson C. 1987 — 5.00
as set with GMS-43 and GMS-45 — 11.00
GMS-45 Madras West/East 7½' quads., Jefferson County. 1987 — 5.00
as set with GMS-43 and GMS-44 — 11.00
GMS-46 Breitenbush River area, Linn and Marion Counties. 1987 — 7.00
GMS-47 Crescent Mountain area, Linn County. 1987 — 7.00
GMS-48 McKenzie Bridge 15' quadrangle, Lane County. 1988 — 9.00
GMS-49 Map of Oregon seismicity, 1841-1986. 1987 — 4.00
GMS-50 Drake Crossing 7½' quadrangle, Marion County. 1986 — 5.00
GMS-51 Elk Prairie 7½' quadrangle, Marion and Clackamas Counties. 1986 — 5.00
GMS-52 Shady Cove 7½' quadrangle, Jackson County. 1992 — 6.00
GMS-53 Owyhee Ridge 7½' quadrangle, Malheur County. 1988 — 5.00
GMS-54 Graveyard Point 7½' quad., Malheur/Owyhee Counties. 1988 — 5.00
GMS-55 Owyhee Dam 7½' quadrangle, Malheur County. 1989 — 5.00
GMS-56 Adrian 7½' quadrangle, Malheur County. 1989 — 5.00
GMS-57 Grassy Mountain 7½' quadrangle, Malheur County. 1989 — 5.00
GMS-58 Double Mountain 7½' quadrangle, Malheur County. 1989 — 5.00
GMS-59 Lake Oswego 7½' quad., Clackam., Multn., Wash. Counties. 1989 — 7.00
GMS-60* Damascus 7½' quad., Clackam., Multn. Counties. 1994 — 8.00
GMS-61 Mitchell Butte 7½' quadrangle, Malheur County. 1990 — 5.00
GMS-62* The Elbow 7½' quadrangle, Malheur County. 1993 — 8.00
GMS-63 Vines Hill 7½' quadrangle, Malheur County. 1991 — 5.00
GMS-64 Sheaville 7½' quadrangle, Malheur County. 1990 — 5.00
GMS-65 Mahogany Gap 7½' quadrangle, Malheur County. 1990 — 5.00
GMS-66 Jonesboro 7½' quadrangle, Malheur County. 1992 — 6.00
GMS-67 South Mountain 7½' quadrangle, Malheur County. 1990 — 6.00
GMS-68 Reston 7½' quadrangle, Douglas County. 1990 — 6.00
GMS-69 Harper 7½' quadrangle, Malheur County. 1992 — 5.00
GMS-70 Boswell Mountain 7½' quadrangle, Jackson County. 1992 — 7.00
GMS-71 Westfall 7½' quadrangle, Malheur County. 1992 — 5.00
GMS-72 Little Valley 7½' quadrangle, Malheur County. 1992 — 5.00
GMS-73* Cleveland Ridge 7½' quadrangle, Jackson County. 1993 — 5.00
GMS-74 Namorf 7½' quadrangle, Malheur County. 1992 — 5.00
GMS-75 Portland 7½' quadrangle, Multn., Wash., Clark Counties. 1991 — 7.00
GMS-76 Camas Valley 7½' quadrangle, Douglas and Coos Counties. 1993 — 6.00
GMS-77 Vale 30×60 minute quadrangle, Malheur County. 1993 — 10.00
GMS-78 Mahogany Mountain 30×60 minute quadrangle, Malheur C. 1993 — 10.00
GMS-79* Earthquake hazards, Portland 7½' quad., Multnomah C. 1993 — 20.00
GMS-80* McLeod 7½' quadrangle, Jackson County. 1993 — 5.00
GMS-81* Tumalo Dam 7½' quadrangle, Deschutes County. 1994 — 6.00
GMS-82* Limber Jim Creek 7½' quadrangle, Union County. 1994 — 5.00
GMS-83* Kenyon Mountain 7½' quadrangle, Douglas/Coos Counties. 1994 — 6.00
GMS-84* Remote 7½' quadrangle, Coos County. 1994 — 6.00
GMS-85* Mount Gurney 7½' quadrangle, Douglas/Coos Counties. 1994 — 6.00
GMS-86* Tenmile 7½' quadrangle, Douglas County. 1994 — 6.00
GMS-87* Three Creek Butte 7½' quadrangle, Deschutes County. 1996 — 6.00
GMS-88* Lakecreek 7½' quadrangle, Jackson County. 1995 — 8.00
GMS-89* Earthquake hazards, Mt. Tabor 7½' quad., Multnomah C. 1995 — 10.00
GMS-90* Earthquake hazards, Beaverton 7½' quad., 1995 — 10.00
GMS-91* Earthquake hazards, Lake Oswego 7½' quad., 1995 — 10.00
GMS-92* Earthquake hazards, Gladstone 7½' quad., 1995 — 10.00
GMS-93* Earthquake hazards, Siletz Bay area, Lincoln County, 1995 — 20.00
GMS-94* Charleston 7½' quadrangle, Coos County. 1995 — 8.00
GMS-97* Coos Bay 7½' quadrangle, Coos County. 1995 — 6.00
GMS-98* Dora and Sitkum 7½' quadrangles, Coos County. 1995 — 6.00
GMS-99* Tsunami hazard map, Siletz Bay area, Lincoln County. 1996 — 6.00
GMS-100* Earthquake hazard maps for Oregon. 1996 — 8.00
GMS-101* Steelhead Falls 7½' quad., Deschutes/Jefferson Co. 1996 — 7.00
GMS-104* Earthquake hazards, Linnton 7½' quad., Multn./Wash. Co. 1996 — 10.00
GMS-105* Earthquake hazards, Salem East/West 7½' quads. 1996 — 12.00

SPECIAL PAPERS

2 Field geology, SW Broken Top quadrangle. 1978 — 5.00
3 Rock material resources, Clackam., Columb., Multn., Wash. C. 1978 — 8.00
4 Heat flow of Oregon. 1978 — 4.00
5 Analysis and forecasts of demand for rock materials. 1979 — 4.00
6 Geology of the La Grande area. 1980 — 6.00
7 Pluvial Fort Rock Lake, Lake County. 1979 — 5.00
8 Geology and geochemistry of the Mount Hood volcano. 1980 — 4.00
9 Geology of the Breitenbush Hot Springs quadrangle. 1980 — 5.00
10 Tectonic rotation of the Oregon Western Cascades. 1980 — 4.00
11 Bibliography and index of theses and dissertations, 1899-1982. 1982 — 7.00
12 Geologic linears, northern part of Cascade Range, Oregon. 1980 — 4.00
13 Faults and lineaments of southern Cascades, Oregon. 1981 — 5.00
14 Geology and geothermal resources, Mount Hood area. 1982 — 8.00
15 Geology and geothermal resources, central Cascades. 1983 — 13.00
16 Index to *Ore Bin* (1939-78) and *Oregon Geology* (1979-82). 1983 — 5.00
17 Bibliography of Oregon paleontology, 1792-1983. 1984 — 7.00
18 Investigations of talc in Oregon. 1988 — 8.00
19 Limestone deposits in Oregon. 1989 — 9.00
20 Bentonite in Oregon. 1989 — 7.00
21 Field geology, NW¼ Broken Top 15' quadrangle, Deschutes C. 1987 — 6.00
22 Silica in Oregon. 1990 — 8.00
23 Forum on Geology of Industrial Minerals, 25th, 1989, Proceedings. 1990 — 10.00
24 Index to Forums on the Geology of Industrial Minerals, 1965-1989. 1990 — 7.00
25 Pumice in Oregon. 1992 — 9.00
26 Onshore-offshore geol. cross section, N. Coast Range to cont. slope. 1992 — 11.00
27 Economic analysis, construction aggregate markets and forecast. 1995 — 15.00

OIL AND GAS INVESTIGATIONS

3 Foraminifera, General Petroleum Long Bell #1 well. 1973 — 4.00
4 Foraminifera, E.M. Warren Coos County 1-7 well. 1973 — 4.00
5 Prospects for natural gas, upper Nehalem River Basin. 1976 — 6.00
6 Prospects for oil and gas, Coos Basin. 1980 — 10.00
7 Correlation of Cenozoic stratigraphic units, W. Oregon/Washington. 1983 — 9.00
8 Subsurface stratigraphy of the Ochoco Basin, Oregon. 1984 — 8.00
9 Subsurface biostratigraphy of the east Nehalem Basin. 1983 — 7.00
10 Mist Gas Field: Exploration/development, 1979-1984. 1985 — 5.00
11 Biostratigraphy of exploratory wells, W. Coos, Douglas, Lane Co. 1984 — 7.00
12 Biostratigraphy, exploratory wells, N. Willamette Basin. 1984 — 7.00
13 Biostratigraphy, exploratory wells, S. Willamette Basin. 1985 — 7.00
14 Oil and gas investigation of the Astoria Basin. 1985 — 8.00
15 Hydrocarbon exploration and occurrences in Oregon. 1989 — 8.00
16 Available well records and samples, onshore/offshore. 1987 — 6.00
17 Onshore-offshore cross section, Mist Gas Field to cont. shelf/slope. 1990 — 10.00
18 Schematic fence diagram, S. Tyee basin, Oregon Coast Range. 1993 — 9.00
19 Oil and gas potential of the S. Tyee Basin, S. Oregon Coast Range. 1996 — 20.00

OREGON GEOLOGY
Suite 965, 800 NE Oregon Street # 28,
Portland, OR 97232-2162

Periodicals postage
paid at Portland, OR

AVAILABLE DEPARTMENT PUBLICATIONS (continued)

BULLETINS

	Price	☑
33 Bibliography, geol. & min. res. of Oregon (1st suppl. 1936-45). 1947	4.00	
36 Papers on Tertiary Foraminifera (v. 2 [parts VII-VIII] only). 1949	4.00	
44 Bibliography (2nd supplement, 1946-50). 1953	4.00	
46 Ferruginous bauxite, Salem Hills, Marion County. 1956	4.00	
53 Bibliography (3rd supplement, 1951-55). 1962	4.00	
65 Proceedings of the Andesite Conference. 1969	11.00	
67 Bibliography (4th supplement, 1956-60). 1970	4.00	
71 Geology of lava tubes, Bend area, Deschutes County. 1971	6.00	
78 Bibliography (5th supplement, 1961-70). 1973	4.00	
82 Geologic hazards of Bull Run Watershed, Multn./Clackam. C. 1974	8.00	
87 Environmental geology, western Coos/Douglas Counties. 1975	10.00	
88 Geology/min. res., upper Chetco R. drainage, Curry/Josephine C. 1975	5.00	
89 Geology and mineral resources of Deschutes County. 1976	8.00	
90 Land use geology of western Curry County. 1976	10.00	
91 Geologic hazards, parts of N. Hood River, Wasco, Sherman C. 1977	9.00	
92 Fossils in Oregon. Collection of reprints from the *Ore Bin*. 1977	5.00	
93 Geology, mineral resources, and rock material, Curry County. 1977	8.00	
94 Land use geology, central Jackson County. 1977	10.00	
95 North American ophiolites (IGCPproject). 1977	8.00	
96 Magma genesis. AGU Chapman Conf. on Partial Melting. 1977	15.00	
97 Bibliography (6th supplement, 1971-75). 1978	4.00	
98 Geologic hazards, eastern Benton County. 1979	10.00	
99 Geologic hazards of northwestern Clackamas County. 1979	11.00	
101 Geologic field trips in W. Oregon and SW. Washington. 1980	10.00	
102 Bibliography (7th supplement, 1976-79). 1981	5.00	
103 Bibliography (8th supplement, 1980-84). 1987	8.00	

MISCELLANEOUS PAPERS

5 Oregon's gold placers. 1954	2.00	
11 Articles on meteorites (reprints from the *Ore Bin*). 1968	4.00	
15 Quicksilver deposits in Oregon. 1971	4.00	
19 Geothermal exploration studies in Oregon, 1976. 1977	4.00	
20 Investigations of nickel in Oregon. 1978	6.00	

SHORT PAPERS

	Price	☑
25 Petrography of Rattlesnake Formation at type area. 1976	4.00	
27 Rock material resources of Benton County. 1978	5.00	

MISCELLANEOUS PUBLICATIONS

Hiking Oregon's geology, E.M. Bishop and J.E. Allen, 1996	16.95	
Assessing earthquake hazards in the Pac. NW (USGS Prof. Paper 1560)	25.00	
Geology of Oregon, 4th ed., E.L. and W.N. Orr and E.M. Baldwin, 1991, published by Kendall/Hunt (add $3.00 for mailing)	33.95	
Geologic map of Oregon, G.W. Walker and N.S. MacLeod, 1991, published by USGS (add $3.00 for mailing)	11.50	
Geology of the Pacific Northwest, E.L. and W.N. Orr, 1996, published by McGraw-Hill (add $3.00 for mailing)	43.00	
Geological highway map, Pacific Northwest region, Oregon, Washington, and part of Idaho (published by AAPG). 1973	8.00	
Oregon Landsat mosaic map (published by ERSAL, OSU). 1983	11.00	
Mist Gas Field map, rev. 1997, with 1993-96 production figs. (OFR O-97-1)	8.00	
Digital form of map (CAD formats .DGN, .DWG, .DXF), 3½-in. diskette	25.00	
Mist Gas Field production figures 1979 through 1992 (OFR O-94-6)	5.00	
Northwest Oregon, Correlation Sec. 24. Bruer & others, 1984 (AAPG)	6.00	
Oregon rocks and minerals, a description. 1988 (OFR O-88-6)	6.00	
Mineral information layer for Oregon by county (MILOC), 1993 update (OFR O-93-8), 2 diskettes (5¼-in., high-density, MS-DOS)	25.00	
Directory of mineral producers, 1993 update, 56 p. (OFR O-93-9)	8.00	
Geothermal resources of Oregon (published by NOAA). 1982	4.00	
Mining claims (State laws governing quartz and placer claims)	Free	
Back issues of *Oregon Geology*	3.00	

Separate price lists for open-file reports, tour guides, recreational gold mining information, and non-Departmental maps and reports will be mailed upon request.

GMS maps marked with an asterisk (*) are available in digital form on diskette (geological information only).

The Department also sells Oregon topographic maps published by the U.S. Geological Survey.

ORDER AND RENEWAL FORM

Check desired publications in list above or indicate how many copies and enter total amount below. Send order to **The Nature of the Northwest Information Center, Suite 177, 800 NE Oregon Street, Portland, OR 97232-2162**, or to **FAX (503) 731-4066**. If you wish to order by phone, have your credit card ready and call **(503) 872-2750**. Payment must accompany orders of less than $50. Payment in U.S. dollars only. Publications are sent postpaid. All sales are final. Subscription price for *Oregon Geology*: $10 for 1 year, $22 for 3 years.

Renewal ___ / new subscription___ to *Oregon Geology*: 1 year ($10) or 3 years ($22) $_____

Total amount for publications marked above: $_____

Total payment enclosed or to be charged to credit card as indicated below: $_____

Name_____

Address_____

City/State/Zip_____

Please charge to Visa__ / Mastercard__, account number: _____

Expiration date: _____

Cardholder's signature_____